Middle Pleistocene vertebrate fossils from the Nefud Desert, Saudi Arabia, and their implications for biogeography and palaeoecology

Christopher M. Stimpson[a†], Adrian Lister[b], Ash Parton[a], Laine Clark-Balzan[a], Paul S. Breeze[c], Nick A. Drake[c], Huw S. Groucutt[a], Richard Jennings[a], Eleanor M.L. Scerri[a], Tom S. White[a], Mathieu Duval[d], Rainer Grün[e], Abdulaziz Al-Omari, A.[f], Khalid Sultan M. Al Murayyi[f], Iyaed S. Zalmout[g], Yahya A. Mufarreh[g], Abdullah M. Memesh[g] and Michael D. Petraglia[a]

[a] School of Archaeology, Research Laboratory for Archaeology and the History of Art, Hayes House, 75 George Street University of Oxford, Oxford OX1 2BQ, UK

[b] Earth Sciences Department, Natural History Museum, London SW7 5BD, UK

[c] Department of Geography, King's College London, Strand, London, WC2R 2LS, UK

[d]Centro Nacional de Investigación sobre la Evolución Humana (CENIEH), Paseo de Atapuerca, 3, 09002-Burgos, Spain

[e]Environmental Futures Research Institute, Nathan campus, Griffith University, 170 Kessels Road QLD 4111, Australia

[f] The Saudi Commission for Tourism and National Heritage, P.O Box 66680, Riyadh 11586, Saudi Arabia

[g] Saudi Geological Survey, Palaeontology Unit, Jeddah 21514, Saudi Arabia

†corresponding author: School of Archaeology, Research Laboratory for Archaeology and the History of Art, First Floor, Hayes House, 75 George Street, Oxford OX1 2BQ.

Tel: +44 (0) 1865 611741

e-mail: christopher.stimpson@rlaha.ox.aca.uk

Abstract

The current paucity of Pleistocene vertebrate records from the Arabian Peninsula - a landmass of over 3 million km^2 - is a significant gap in our knowledge of the Quaternary. Such data are critical lines of contextual evidence for considering animal and hominin dispersals between Africa and Eurasia generally, and hominin palaeoecology in the Pleistocene landscapes of the Arabian interior specifically. Here, we describe an important contribution to the record and report stratigraphically-constrained fossils of mammals, birds and reptiles from recent excavations at the site at Ti's al Ghadah in the southwestern Nefud Desert. U series and combined US-ESR analyses of *Oryx* sp. teeth indicate that the assemblage is Middle Pleistocene in age and dates to ca. 500 ka. The identified fauna is a biogeographical admixture that consists of likely endemics and taxa of African and Eurasian affinity and includes extinct and extant (or related Pleistocene forms of) mammals (*Palaeoloxodon* cf. *recki*, *Panthera* cf. *gombaszogenis*, *Equus hemionus*, cf. *Crocuta crocuta*, *Vulpes* sp., *Canis anthus, Oryx* sp.), the first Pleistocene records of birds from the Arabian Peninsula (*Struthio* sp., *Neophron percnopterus, Milvus* cf. *migrans*, *Tachybaptus* sp. *Anas* sp., *Pterocles orientalis*, *Motacilla* cf. *alba*) and reptiles (Varanidae/*Uromastyx* sp.). We infer that the assemblage reflects mortality in populations of herbivorous animals and their predators and scavengers that were attracted to freshwater and plant resources in the inter-dune basin. At present, there is no evidence to suggest hominin agency in the accumulation of the bone assemblages. The inferred ecological characteristics of the taxa recovered indicate the presence, at least periodically, of substantial water-bodies and open grassland habitats.

Keywords: vertebrates, Pleistocene, desert, Saudi Arabia, lacustrine, palaeoecology, biogeography

1. Introduction

The Arabian Peninsula (defined here as the landmass from the southern borders of Iraq and Jordan, to the southern coastline of Yemen; **Fig. 1A**) is a key theatre to consider hominin dispersals between Africa and Eurasia (e.g. Dennell and Petraglia, 2012; Groucutt and Petraglia, 2012; Rose and Petraglia, 2010). While the geographical significance of this landmass of over 3 million km^2 as a link between these continents is self-evident, the potential routes and timing of dispersals and exchange by animals and hominins in the Pleistocene (2.6 Ma to 0.011 Ma) are much-debated (e.g. Beyin, 2006; Fernandes, 2009; Fernandes et al., 2006; Groucutt et al., 2015a; O'Regan et al., 2005, O'Regan et al., 2011).

As studies continue to unveil a complex climatic and environmental history (e.g. Breeze et al., 2015; Fleitmann and Matter, 2009; Fleitmann et al., 2003; Fleitmann et al., 2011; Jennings et al., 2015; Matter et al., 2015; Parker, 2009; Parton et al., 2015a; Parton et al., 2015b; Rosenberg et al., 2011; Rosenberg et al., 2013) and the Palaeolithic archaeological record develops (e.g. Armitage et al., 2011; Delagnes et al., 2012; Delagnes et al., 2013; Groucutt and Petraglia, 2012; Petraglia et al., 2012) it is now clear that Pleistocene hominins penetrated the interior of the Peninsula (Groucutt et al., 2015b; Groucutt et al. 2015c; Scerri et al., 2015; Shipton et al., 2014) in regions that are today harsh, hyper-arid habitats. A key line of evidence to contextualise these movements is, however, lacking: stratigraphically- and chronologically-constrained records of vertebrates. Here, we describe an important step towards addressing this issue.

North Africa and the Middle East are biogeographically complex regions. The Arabian Peninsula is situated at the junction of three biogeographic realms, the Afrotropical, Western Paleartic and Oriental (e.g. Portik and Papenfuss, 2012) and the historical vertebrate fauna is an admixture of endemic species with taxa of African and Eurasian affinity (e.g. Cox et al., 2012; Delany, 1989; Harrison and Bates, 1991; Portik and Papenfuss, 2012). The opening of the Red Sea and climatic shifts in the late Miocene were major drivers of diversification and dispersal of the biota of the region and a combination of harsh arid environments, periodic humid events and geological evolution has shaped the fauna of the Peninsula (e.g. Metallinou et al., 2012). Genetic studies of a small number of species (*Papio hamadryas, Ichneumia albicauda* and *Varanus yemenensis*) have shed light on the biogeographical history of aspects of the regional Pleistocene fauna (Fernandes, 2009 and Kopp et al.,

2014; Fernandes, 2011; Portik and Papenfuss, 2012, respectively) but, in contrast to works on Miocene vertebrates (e.g. Whybrow and Hill, 1999; Beech and Hellyer, 2005), the paucity of Pleistocene records from the Arabian Peninsula remains a major limiting factor in modelling the dynamics of Quaternary animal populations (e.g. Fernades, 2009; O'Regan et al., 2011; Stimpson et al., 2015). Furthermore, while records of vertebrate taxa cannot be considered as direct or unequivocal proxies for the dispersal of hominins (e.g. Bar-Yosef and Belmaker, 2011) and species responses to climatic and environmental changes are individualistic (e.g. Stewart, 2009), such data are critical lines of contextual evidence in considering Pleistocene environments and hominin palaeoecology in the interior (e.g. Belmaker, 2009).

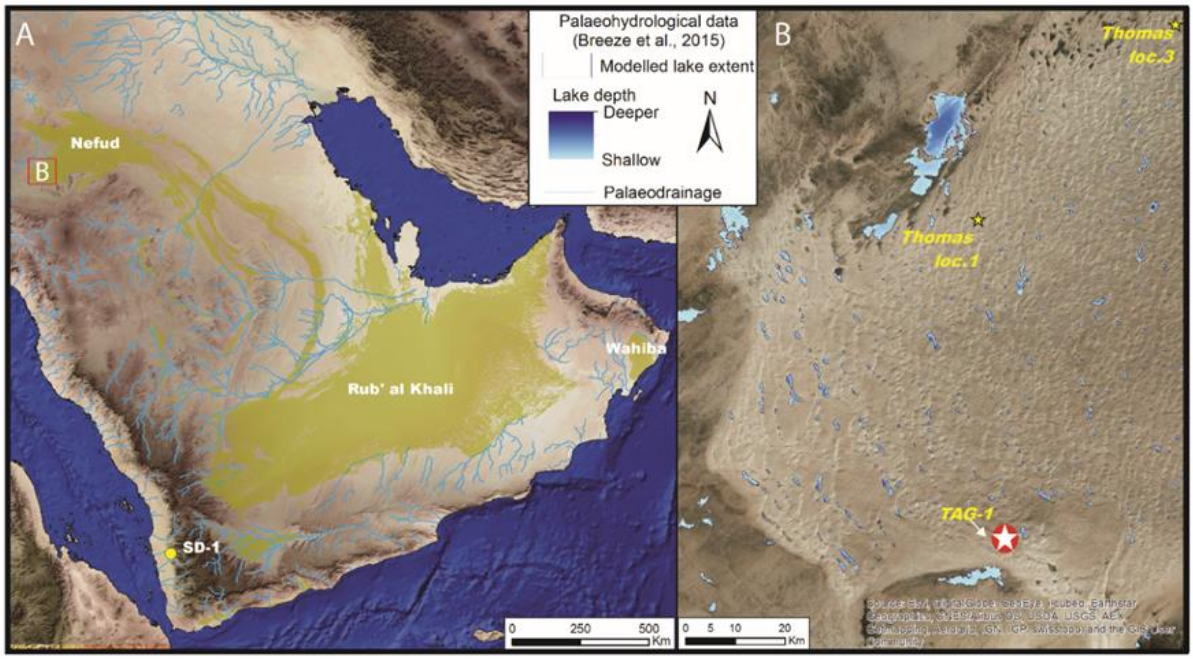

Fig. 1. A: The Arabian Peninsula and B: location of Ti's al Ghadah (TAG-1) and Thomas et al. (1998) fossil sites in the southwestern Nefud.

The Arabian Peninsula today comprises of a heterogeneous suite of habitats, including tropical, sub-tropical and montane biomes in the south and western coastal regions. The interior, however, is dominated by basalt flows, salt flats and (overwhelmingly) sand and gravel deserts (Cox et al., 2012; Mallon, 2011). These hyper-arid habitats are embodied by three major sands seas that collectively occupy over 700,000 km^2: the Rub' al Khali (also known as the Empty Quarter) and Wahiba Sands in the south and southeast, respectively, and the Nefud Desert in the north (**Fig. 1A**). During the Pleistocene, oscillations between hyper-arid and humid conditions saw periodic increases in

precipitation, humidity and the activation of river and lake systems in the interior (Breeze et al., 2015; Matter et al., 2015; Parker, 2009; Parton et al., 2015b; Rosenberg et al., 2013; **Fig. 1A, B**). As the volume and periodicity of available moisture increased plant biomass will have responded accordingly (e.g. Southgate et al., 1996) and an availability of fresh water resources would have led to a "greening" of the interior that in turn would have provided windows of opportunity for dispersal for animals and hominins (e.g. Parton et al., 2015a). However, the character and composition of the animal populations of these landscapes is poorly known. The existing collections of Pleistocene fossils have provided taxonomic insights (**Table 1)** but are beset by problems of preservation, provenance and chronological control (O'Regan et al., 2011; Stimpson et al., 2015).

Excavations of the Late Pleistocene site Shi'bat Dihya (SD-1) in Yemen, dated to 55 ka, recovered poorly preserved assemblages of bone (Delagnes et al., 2012). Remains of the post-cranial skeleton were impossible to identify. Tooth fragments could be assigned to four mammalian families: Bovidae, Suidae, Hystricidae and Equidae. A tentative identification of Asiatic wild ass (cf. *Equus hemionus*) was proposed from an intact third molar.

Pleistocene fossils have also been recovered from the two largest sand seas of in the interior: the Rub' al Khali and the Nefud Desert (**Fig. 1A**). Collections made by McClure (1984) during pioneering studies of lacustrine deposits in the Rub' al Khali resulted in confident identifications of *Oryx* ("presumably *leucoryx*"), *Bos* (cf. *primigenius*), *Equus* (cf. *hemionus*), *Gazella* sp. ("apparently *G. arabica*"), *Bubalus* sp. and *Hippopotamus* ("presumably *amphibious*"). Remains of the Caprinae included a possible record of the endemic *Hemitragus* (*Arabitragus*) *jayakari*. McClure points out, however, that collection was not systematic and information for exact geographical provenance and chronological affinities of the fossil assemblages was lacking. Essentially, the "fossil vertebrate suite should therefore be taken as representing the general lacustrine periods of both late Pleistocene and Holocene" (McClure, 1984, 179) with the proviso that it was likely that the hippopotamus and large water buffalo "belong to the earlier (Late Pleistocene) period" (McClure, 1984, 181).

In the north of the Peninsula, Pleistocene fossils are known to be associated with lacustrine deposits in the Nefud Desert (Rosenberg et al., 2013; Thomas et al., 1998). Thomas and colleagues (1998) reported the first Pleistocene fossil collections from a survey of three sites in the southwestern

Nefud Desert (including the site at Ti's al Ghadah, the focus of this study; **Figs. 1B, 2**). Despite relatively small sample sizes, a total of 14 taxa (including fish, reptiles and mammals) were identified (**Table 1**).

Table 1

Pleistocene vertebrate taxa from the Arabian Peninsula reported prior to this study. Sources: Shi'bat Dihya - taxa and dates, Delagnes et al. (2012); Rub' al Khali - taxa, McClure (1984); Nefud Desert - taxa[a], Thomas et al. (1998), taxa[b], Stimpson et al. (2015), dates, Rosenberg et al. (2013). X = present; / = no record.

REGION	**Southwest**	**Rub' al Khali**	**Nefud Desert**			
SITES	Shi'bat Dihya (SD-1)	lacustrine deposits	Khall Amayshan (Thomas loc-1)	Ti's al Ghadah (TAG-1)		"Locality #3" (Thomas loc-3)
DATES (ka)	55	/	99±7/117±8	318±25/328±26		419±39 to 286±30
Inferred MIS	3	1-3?	5c/5e	9		9-11
TAXA				**a**	**b**	
ACTINOPTERYGII						
Osteoglossiformes	/	/	/	X	/	/
SAUROPSIDA						
Geochelone cf. *sulcata*	/	/	/	X	/	/
REPTILIA						
Squamata	/	/	/	/	X	/
AVES						
Tachybaptus sp.	/	/	/	/	X	/
MAMMALIA						
Equus sp.	/	/	X	X	/	/
cf. *E. hemionus*	X	X	/	/	/	/
cf. *Palaeoloxodon (recki)*	/	/	/	/	X	X
cf. *Hexaprotodon* sp.	/	/	X	/	/	/
Hippopotamus sp.	/	X	/	/	/	/
Suidae: gen. et sp. indet.	X	/	/	/	/	/
Panthera cf. *gombaszogensis*	/	/	/	X	X	/
Vulpes (cf. *vulpes*)	/	/	/	X	X	/
Crocuta crocuta	/	/	/	/		X
Bovidae: gen. et sp. indet.	X	/	/	X	/	X
Pelorovis (cf. *oldowayensis*)	/	/	X	/	/	X
Bos cf. *primigenius*	/	X	/	/	/	/
Bubalus sp.	/	X	/	/	/	/
Oryx sp.	X	X	/	X	X	/
Gazella sp.	/	X	/	/	/	/
cf. *Arbitragus jayakari*	X	/	/	/	/	/
Camelidae gen. et sp. indet.	/	/	/	X	/	/

The site at Khall Amayshan (KAM-1 – Thomas locality 1; **Fig. 1B**) yielded fossils of *Equus* sp., a large bovid (identified as *Pelorovis* cf. *oldawayensis*) and a reportedly gracile hippopotamid

(*Hexaprotodon* sp.?) that, upon review, is more likely to be *Hippopotamus* sp. (White et al., forthcoming). Fossils from an unnamed site ("Locality 3" in Thomas et al., 1998; **Fig. 1B**) that is likely site 16.1 of Rosenberg et al. (2013), which yielded OSL dates between 419 ± 39 ka and 286 ± 30 ka, included large bovids (referred to *Pelorovis* cf. *oldawayensis*), a well preserved left mandible of *Crocuta crocuta*, and post-crania and a molar from an elephant. Examination of the incomplete, hypsodont molar plate resulted in a cautious referral to the extinct African elephant taxon *Palaeoloxodon recki*. An aberrant horn-core (originally reported to be from Ti's al Ghadah) that possibly represented an undescribed taxon was also recovered from this site.

The site at Ti's al Ghadah (**Fig. 2**) yielded the largest and most diverse sample. The collection included a relative abundance of fossils from *Oryx* sp. together with small numbers of specimens attributable to tortoise (*Geochelone* cf. *sulcata*), a large Osteoglossiforme fish (a specimen we were unfortunately unable to relocate and review), *Equus* sp., *Vulpes* sp. and a specimen conferred to the extinct Eurasian jaguar, *Panthera (onca) gombaszogensis* (see also Stimpson et al., 2015). Unidentified, potentially novel bovid and camelid taxa were also reported. Re-inspection of the bovid remains from the collection at Ti's al Ghadah by one of us (CMS) suggested that the crania may be attributable to a Pleistocene *Oryx* sp. (see also section **4.2.3.4**). A poorly preserved maxilla fragment appears to be camelid, but with no discernible difference to extant *Camelus*.

While these collections provide some insight into the Pleistocene vertebrates of the interior, they were the product of surface collections and their stratigraphic and chronological affinities are not clear (Stimpson et al., 2015). In the original report these collections were considered as a whole and an Early Pleistocene age and an Ethiopian affinity were inferred on the basis of taxonomic composition and "stage of evolution" (Thomas et al., 1998, 150). Subsequent dating work by Rosenberg et al. (2013) using luminescence techniques at these fossil localities indicated that this fauna was younger and derived from different temporal episodes and incorporated fossils of likely Middle and Late Pleistocene age (**Table 1**). As such, further work to resolve the identity and chronological affinities of the Nefud fauna is warranted.

Here we describe an important step towards resolving the character and chronological context of the Pleistocene vertebrates of the Nefud Desert. Following collaborative investigations of the fossil

site of Ti's al Ghadah by the Saudi Commission for Tourism and National Heritage (SCTH), Saudi Geological Survey (SGS) and the Palaeodeserts project (University of Oxford), we describe stratigraphically-constrained records of mammals, birds and reptiles. We report the results of our chronometric and stratigraphic investigations and consider the biostratigraphic and palaeoecological, and palaeoenvironmental implications of the identified taxa.

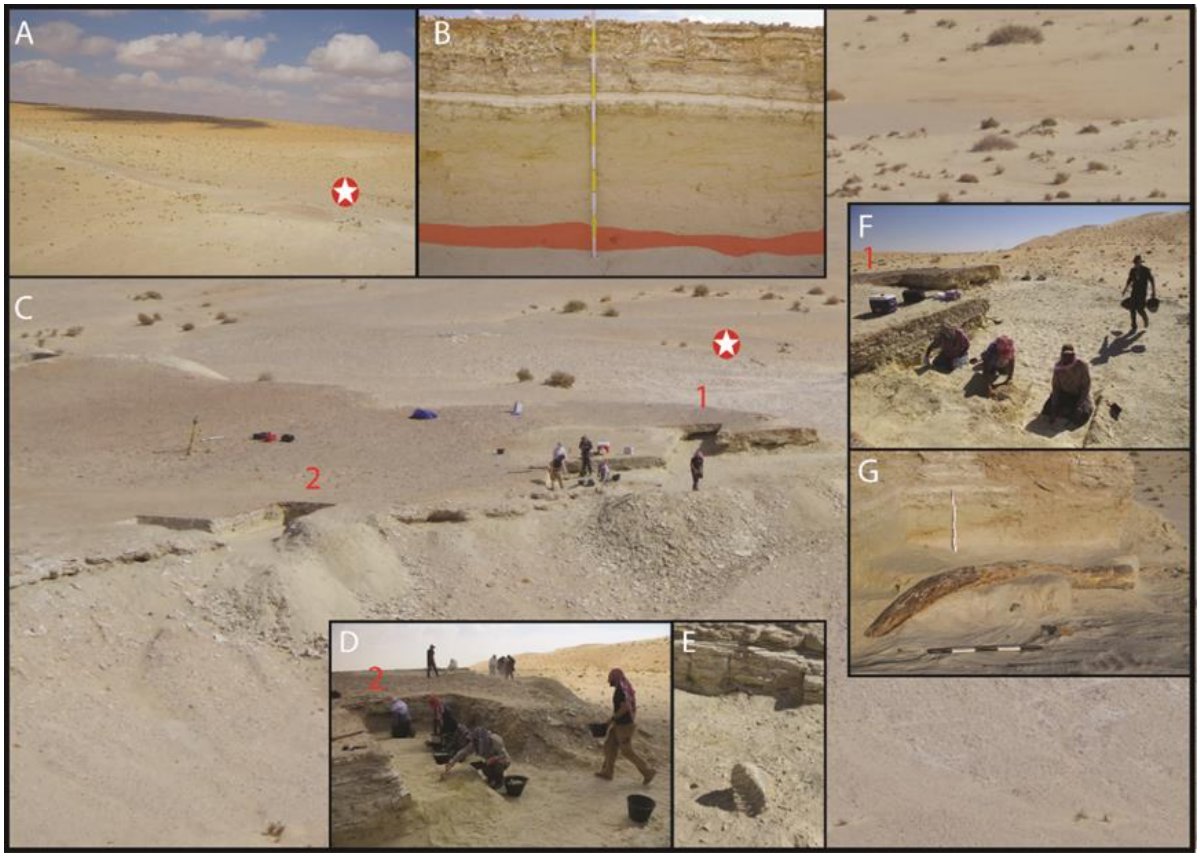

Fig. 2. The fossil site of Ti's al Ghadah. A: the ridge viewed from the southwest from the adjacent barcan dune. B: Section through the ridge deposit after excavation (scale = 10 cm increments: the position of the fossil layer within Unit 5 is highlighted in red). C: Excavation of trenches 1 and 2 (numbered in red) at the southern end of the ridge, viewed from the southwest. D: Excavation of trench 2, viewed from the west. E: TAG14/301 - *Palaeoloxodon* molar, in situ in trench 2. F: Excavation of trench 1, viewed from the north. G: TAG13/052 – elephant tusk, in situ in trench 1.

2. Site location and geological setting

The site at Ti's al Ghadah is situated within an interdunal basin in the southwest of the Nefud Desert, approximately 95 km southeast of the city of Tayma (**Fig. 1B**). The basin is bordered to the west by a

large (ca. 60 m high) compound barchan dune ridge, while smaller branching linear dunes extend to the northern and southern ends of the basin. Relict lacustrine deposits form a distinct ridge that runs broadly northwest to southeast (**Figs. 2A, 3**). This ridge is comprised of a sequence of stratified sands and marls (**Fig. 2B**) that rises approximately 6 m above the floor of the basin, and is approximately 1 km in length. It dips gently to the south of the basin and interdigitates with low branching dunes in the east. Lacustrine and diatomaceous marls are exposed vertically along the western edge of the ridge (**Fig. 2C**) and dip gently to the east where they are overlain by modern dune sands. Ephemeral gullies run perpendicular to the long axis of the ridge towards the west of the basin and at the foot of the large barchan dune. These have eroded fossils from the main lake ridge, re-depositing them unconformably downslope in sinuous ridges comprised of heavily indurated, coarse, red-brown sand. Pale cream-grey sands are exposed along the southeastern corner of the basin, and represent an older palaeodune configuration that lies beneath the present day rubified sand sea. Exposed within the centre of the basin, are heavily indurated, iron-stained marl beds ca. 0.6 m thick, reflecting the formation of an older lake that predates the main lake ridge deposit. Conversely, at the northwestern edge of the basin, thin (ca. 0.4 m) beds of diatomaceous marls outcrop from the smaller branching linear dunes and represent a phase of lake formation that postdates the formation of the main lake ridge. The lacustrine silts and diatomaceous marls of the ridge have formed an armoured cap to the thick beds of interdigitated sands that lie beneath, including the principal fossiliferous deposit: Unit 5.

3. Materials and Methods

3.1 Excavation

Excavations on the ridge focused on Unit 5 (Fig. 2A-H; Fig. 4): methodology is described in Stimpson et al. (2015). The general lithofacies described in Stimpson et al. (2015; n.b. Unit 5 = "Layer 5") were found throughout the excavations with major variation between trenches limited to the relative thickness of the lacustrine deposit and the greenish grey sands overlying Unit 5. All overlying deposits were removed following stratigraphic boundaries and all fragments in Unit 5 were collected. The locations of diagnostic specimens (> 5 mm in maximum dimension with anatomical landmarks) were recorded in three dimensions by Leica Flexline Total Station (**Fig. 5A**).

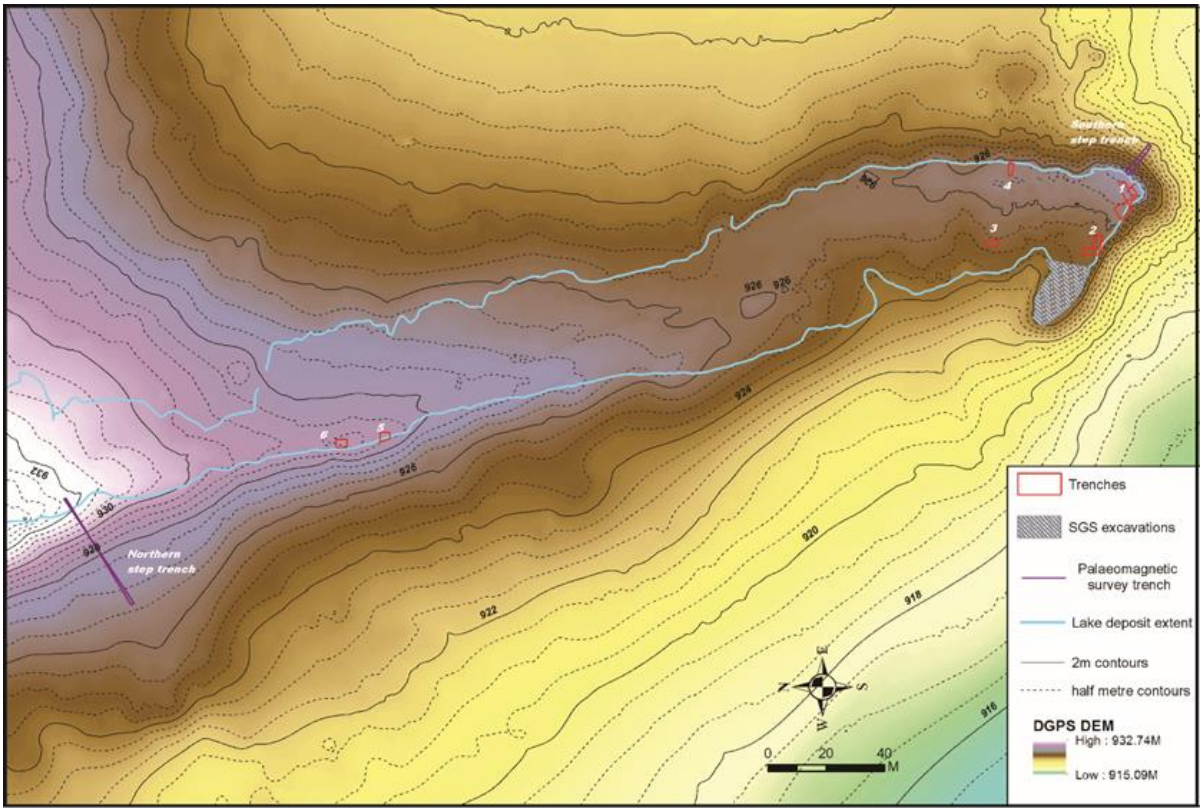

Fig. 3. Plan view of the ridge at the fossil site of Ti's al Ghadah, showing location of trenches.

Searches for possible, earlier fossil-bearing strata in the ridge and in the wider basin area were made by the creation of step trenches in the north and south of the ridge (**Fig. 3**) and a series of test pits in the basin. While the deep section exposed by the step trenches provided further sedimentological information regarding the geomorphological evolution of the basin, no further fossiliferous layers were detected.

3.2 Fossil analyses

The identification of the fossils was conducted in the UK with the permission of the SCTH. Fossils were identified by morphological and morphometric comparisons with comparative museum specimens, published descriptions and morphometric data. Measurements of bones generally follow the schemes described in Von den Driesch (1976), and for elephant molars Maglio (1973) but are defined in the text. Measurements were taken with dial callipers to the nearest 0.01 mm. Morphometric analyses were carried out in PAST (Hammer et al., 2001) following conventions described in Hammer et al.

(2006). A preliminary macroscopic taphonomic investigation was conducted and surface condition and modifications to bones were noted. Weathering stages were characterised following Behrensmeyer (1978) and interpreted following Andrews and Whybrow (2005).

For mammals and reptiles, modern reference materials were consulted at the Oxford University Museum of Natural History (OUMNH), the Graeme Clark Zooarchaeology Laboratory, University of Cambridge (GCZL) and the Harrison Zoological Institute (HZM). Palaeontological specimens and modern comparatives were also consulted at the Department of Earth Sciences at the Natural History Museum (South Kensington – NHM-SK). For birds, recent comparative materials were consulted at the Bird Group, Natural History Museum (Tring- NHM-T) and palaeontological comparative specimens at the NHM-SK.

3.3 Chronology

A sample for OSL dating was recovered from a stratum that directly underlies, or is equivalent to the main bone-bearing layer (Units 4 or 5, respectively; Fig. 4) by Rosenberg et al. (2013). This sample yielded OSL and TT-OSL (thermally-transferred optically stimulated luminescence) ages of 328 ± 26 ka and 318 ± 25 ka, respectively. The overlying lake formation was interpreted as an MIS 9 deposit (Rosenberg et al., 2013).

To refine our understanding of the chronology of the lacustrine deposit and the fossiliferous stratum that underlies it, we sampled the lake deposit for OSL dating (Unit 7) and five fossil cheek teeth (*Oryx* sp.) that were recovered from Unit 5 were submitted for U-series and combined US-ESR dating (**Table S1 supplementary data**). Additionally, a series of sediment samples were collected from different depths within Unit 5 to evaluate the variability of the sediment radioactivity.

3.3.1 Optically Stimulated Luminescence

One sample for luminescence dating was collected from the palaeolake sediments capping the excavated sequence (Unit 7; **Fig. 4**). A metal tube was hammered into a cleaned section, capped, and transported to the Research Laboratory for Archaeology and the History of Art (University of Oxford) for preparation and measurement. Coarse-grained potassium feldspars (180-255 μm) were extracted

from the consolidated sample via hydrochloric acid treatment, wet sieving, and density separation with sodium polytungstate ($\rho < 2.58$ g cm-3). Luminescence measurements were conducted with the *lexsyg smart*, a smaller and simpler version of the *lexsyg research* TL/OSL reader (Richter et al., 2013). Infrared stimulation was provided by LEDs emitting 850 ± 20 nm (-- mW cm-^{2}) and emissions were detected with a standard bi-alkaline cathode PMT (Hamamatsu) with peak sensitivity at 420 nm. The *lexsyg smart* incorporates a 90Sr/90Y beta 'flat source' with a dose rate ~0.15 Gy s-1.

Equivalent doses were measured for ten multigrain feldspar aliquots (1 mm diameter) via the single aliquot regeneration (SAR) post-IR, IR stimulation at 290ºC (pIRIR290) protocol (Thiel et al., 2011). This protocol includes recycling and thermal transfer ('zero dose') tests. Net signals were calculated by integrating the first two seconds of emission and subtracting an average background found from the last 50 s. Aliquots were accepted if their recycling ratios were within 10% of unity or overlapped unity at two sigma uncertainty, and if the zero dose step yielded a signal less than 5% of the normalized natural signal or was indistinguishable from 0 at two sigma. Saturated aliquots that passed these two criteria were also rejected from the population used to calculate the luminescence age. Equivalent doses were calculated with Luminescence Analyst v. 4.11, and the central age model was used to calculate overdispersion values and the population De for age determination (Galbraith et al., 1999). The reported ages have not been corrected for fading (Thiel et al., 2010; Thomsen et al., 2011).

External alpha, beta, and gamma dose rates were calculated from elemental concentrations obtained from homogenized sample sediment via ICP-MS analysis (Activation Laboratories, Ltd., Canada). For internal dose rate calculations, grains are assumed to contain 12.5 ± 0.5% potassium (Huntley and Baril, 1997) and 400 ± 100 ppm rubidium-87 (Huntley and Hancock, 2001). Dose rate conversion factors were obtained from Adamiec and Aitken (1998) for potassium, thorium, and uranium. Grain attenuation for these elements was calculated for alpha and beta dose rates according to Brennan et al. (1991) and Brennan (2003), respectively. The internal absorbed dose rate from rubidium was taken directly from Readhead (2002). This results in an internal feldspar dose rate of 0.91 ± 0.15 Gy ka-1. The external dose rate was corrected according to Zimmerman (1971) for sediment water content assuming a burial average of 5 ± 3 % (water/wet sediment). Cosmic dose rates were

calculated using the modern day burial depths, corrected for geomagnetic latitude and altitude (Prescott and Stephan, 1982, Prescott and Hutton, 1988 and Prescott and Hutton, 1994).

3.3.2 U-series analysis of teeth

Laser ablation U-series analyses were carried out at the Research School of Earth Sciences of the Australian National University (Australia), using a custom-built laser sampling system interfaced between an ArF Excimer laser and a MC-ICP-MS Finnigan Neptune (for details, see Eggins et al., 2003; Eggins et al., 2005), following principles and procedures described in Grün et al. (2014). Enamel and dentine of teeth were analysed along separate lines. No individual age calculation was carried when the U-concentrations were below about 0.5 ppm and/or detrital ^{232}Th was observed (elemental U/Th ratios below 300). The analytical data of the enamel and dentine sections were integrated to provide the data input for the ESR age calculations.

3.3.3 Combined US-ESR dating of fossil teeth

Fossil teeth were prepared following a standard ESR dating procedure for enamel powder (e.g. Duval et al., 2011): the enamel layer was mechanically separated from the other dental tissues and both inner and outer surfaces were removed with a dentist drill to eliminate the volume that received an external alpha dose. The samples were then ground and sieved to recover the size fraction of <200 µm. Dose evaluation utilised the multiple aliquot additive dose method. The powder was split into several aliquots and irradiated up to 4019 Gy with a Gammacell1000 Cs-137 gamma source. ESR measurements were carried out with a Bruker Elexsys 500 spectrometer at the Research School of Earth Sciences (RSES) of the Australian National University, using the following acquisition parameters: 3–5 scans, 2 mW microwave power, 1024 points resolution, 12 mT sweep width, 50 kHz modulation frequency, 0.1 mT modulation amplitude, 20 ms conversion time and 5 ms time constant. The ESR intensities were extracted from T1-B2 peak-to-peak amplitudes of the ESR signal (Grün, 2000), and then normalised on the number of scans and mass. All aliquots of a given sample were measured within a short time interval (<1 h). This procedure was repeated twice over two successive days without removing the enamel from the ESR tubes between measurements in order to evaluate measurement precision and thus D_E

reproducibility: the latter was found to be excellent, with a variability of <2% between the two repeated measurements.

For dose evaluations, fitting procedures were carried out with the Microcal OriginPro 9.1 software using a Levenberg-Marquardt algorithm by chi-square minimisation. Data were weighted by the inverse of the squared ESR intensity ($1/I^2$) (Grün and Brumby, 1994). Final equivalent dose (D_E) values were obtained by fitting a single saturating exponential (SSE) through the pooled ESR intensities obtained from the two repeated measurements. Given the magnitude of the D_E values (>2000Gy), a maximum irradiation dose (D_{max}) of 4019 Gy was used, so that D_{max}/D_E ratio remains around 1 as recommended by Duval and Grün (2016) to ensure reliable fitting. The final dose response curves (DRCs) are shown in **Fig. S1 (supplementary data).**

For the dose rate calculations, the following parameters were used: an alpha efficiency of 0.13±0.02 (Grün and Katzenberger-Apel, 1994), Monte-Carlo beta attenuation factors from Marsh (1999), dose-rate conversion factors from Guérin et al. (2011), an estimated water content of 5±3 wt.% in dentine and 10±5 wt.% in sediment. U and Th and K concentrations in raw sediment were determined by ICP-OES and ICP-MS analysis on samples collected within Unit 5 (**Table S2 supplementary data**). The mean radioelement concentration values were used for the age calculations.Combined US-ESR ages were calculated with DATA, a DOS-based programme (Grün, 2009) using the US model defined by Grün et al (1988). Further details about this dating method applied to fossil teeth may be found in Duval (2015).

4. Results

4.1 Stratigraphy, bone distribution and taphonomy

The deepest sedimentary sequence uncovered at the site comprised a total of 9 stratigraphic units (**Fig. 4**), and is underlain by coarse, well-cemented, cross-bedded, pale cream-grey sands (Unit 1). These contain occasional calcareous nodules and iron-stained root impressions throughout the upper ca. 0.6 m of the unit. Unit 2 comprises weakly horizontally bedded, pale cream-white, coarse, poorly sorted sands, which feature iron staining and occasional root voids infilled with coarse, dark brown sand. Granulitic inclusions of well-rounded quartz occur throughout the unit, which displays a diffuse contact

with both the overlying and underlying units. This is overlain by a thin layer (Unit 3) of very poorly sorted greenish sands with no bedding structures and numerous, well-rounded quartz pebble inclusions. The unit is heavily cemented and calcritized at the base, with iron staining and iron-stained root voids throughout. Unit 4 comprises pale cream-grey, very poorly sorted, coarse, horizontally bedded sands. Bedding is variable, being generally weak throughout, but strongly bedded and cemented in places. Vertical and horizontal iron-stained root impressions occur throughout, along with numerous well-rounded quartz granules and small (< 10 mm) pebbles. There is a notable increase in iron staining at the base of the unit, along with generally coarser clasts, while a diffuse contact is present with both over and underlying units.

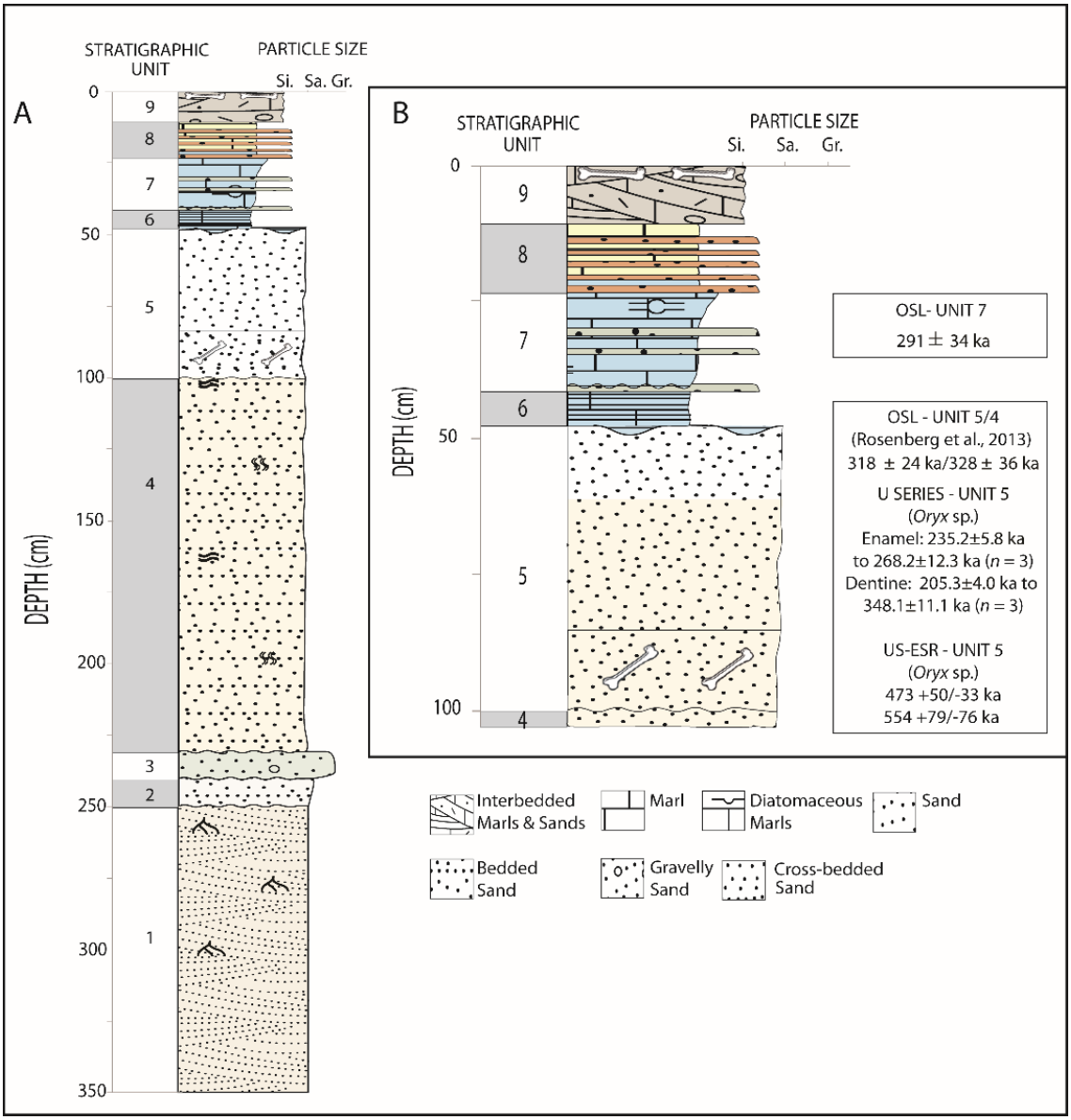

Fig. 4. A: Stratigraphic log of the ridge deposits at Ti's al Ghadah with, B: upper metre of section annotated with OSL and US/ESR dates.

Unit 5 is the main fossil layer at the site and comprises weakly cross-bedded, very poorly sorted, coarse, reddish sands with occasional iron-stained root voids, fine (ca. 5 -10 mm max length) rounded quartz pebbles, and calcareous drapes throughout. The unit becomes notably redder up-profile, while the contact with the overlying unit is characterised as sharp and laterally variable, with marl chunks and fractured laminae intruding vertically from the overlying lake beds. The unit is indicative of the small-scale, localised mobilisation of waterlain sands, displaying evidence of both bioturbation and sediment reworking in the form of small (< 20 cm) infills. Unit 5 is representative of wetted and partially vegetated sands. The characteristics of the underlying unit (Unit 4) indicate initial sediment deposition under low energy (localised) sheetflood conditions, following increased rainfall in the basin. A lack of channel incisions or large clasts throughout the sequence precludes major sediment mobilisation, and is more indicative of continual localised slopewash events. This phase of surface water and sediment mobilisation culminated in the development of vegetation and stabilisation of the landscape represented by Unit 5.

Fossil specimens were mineralised and ranged from a pale, yellowish-brown to (more frequently) a dark reddish-brown: iron-staining was prevalent the latter resulting from the leaching and downward percolation of iron derived from Fe-rich sands within the overlying sedimentary units. Consolidated sand particles were frequently adhered to the bone surface, though were relatively easy to remove with brush or wooden pick. Post-depositional movement and reworking appears to be have been minimal. While minor abrasion was occasionally observed, there was no evidence to suggest rolling or significant water transport. As a general rule, there was a contrast in the degree of weathering between the area of bone in contact with the substrate (less abraded), as exposed during excavation, than the upper surface that was presumably exposed prior to burial (more abraded). Some trampling was evident in the form of the presence of fine stria on the surfaces of bones and "sharp breaks" to specimens (e.g. see **Fig. 15F, H** and **J**). In addition to direct physical evidence of the presence of predators and scavengers on site, carnivore pits and tooth marks indicate the activity of small and large-bodied

carnivores. Tooth marks were identified in the small sample of recovered bird bones (**section 4.2.2**) and were detected on the bones of *Equus* sp. (**4.2.3.2**) and *Oryx* sp. (**section 4.2.3.4**). No lithics were recovered during our excavations and the association between the artefacts reported previously in the basin (Scerri et al., 2015) and the fossiliferous strata remains unclear.

Within the limits of our investigations, there was lateral variation in taxonomic diversity and in the preservation of the recovered specimens between the northern and southern limits of the excavations (**Fig. 3**). Fossils attributable to the Bovidae were numerically dominant throughout although trenches in the south of the site (trenches 1 and 2) yielded a greater range of taxa compared with the northern excavations (trenches 5 and 6; **Fig. 5A**). Weathering profiles generated from examination of bovid long bones from trenches 1,2 and 5 and 6 (**Fig. 5B and 5C, respectively**) indicate that specimens from the south of the site were generally well-preserved: maximally to Behrensmeyer's (1978) weathering stage 3, rarely to stage 4 (**Fig. 5B**). Conversely, specimens from the northerly trenches were paler in colour, more friable and weathering profiles suggest that these specimens were subject to sub-aerial weathering for longer than in the southern trenches (**Fig. 5C**). Following Andrews and Whybrow (2005), the weathering profiles collectively suggest that carcasses were exposed maximally (in arid conditions) for approximately 15 years before burial. However, if conditions were more humid at the time of deposition then the duration of exposure would likely have been less (Behrensmeyer 1978; Andrews and Whybrow, 2005).

The overlying unit (Unit 6) marks the onset of lake formation in the sequence, and comprises a series of interstratified, finely laminated diatomaceous marls. Iron staining occurs throughout, and is prevalent between laminae, however, Fe content is not associated with sand content. Lenses of greenish mark an influx of sand into the basin. These are generally laterally variable and well cemented in places (Unit 7). Unit 8 comprises a series of interdigitated sands and marls, possibly reflecting variations in lake water levels in the basin. Marls are highly cemented and gypsiferous, while sand content is coarse and non-laminar. The sequence is capped by beds of sandy, gypsiferous marls (Unit 9). These are heavily indurated and unevenly bedded in desiccation 'curls'; blocks of marl that have undergone polygonal cracking as a result of drying, and have deformed to make bowl-shaped structures. These are interdigitated due to the extent of deformation, and are predominantly infilled with sand and infrequent

fossil fragments (that have not yet been studied in detail). The unit marks the final phase of drying at the site and desiccation of the lake that forms the main ridge in the basin.

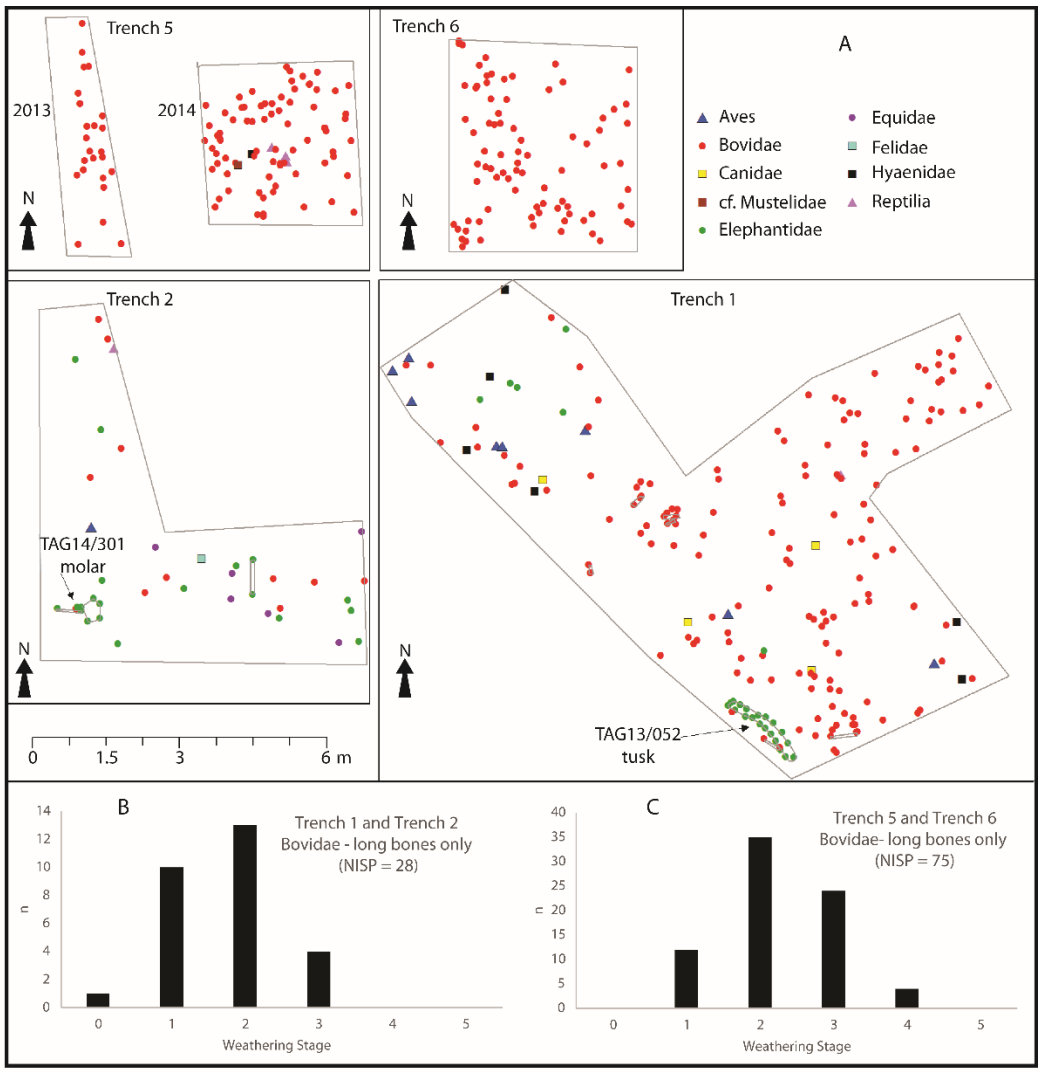

Fig. 5. A: Plots of fossil locations in western trenches 1, 2, 5 and 6, with cumulative weathering profiles (long bones - Bovidae) for B: trenches 1 and 2 and, C: trenches 5 and 6 at Ti's al Ghadah.

4.2 Vertebrate Palaeontology

4.2.1 Reptila

While a small fragment of carapace was recovered from the surface of the ridge deposit (Unit 9), no remains of the Testudinidae have been identified in the excavated materials from Unit 5 (cf. Thomas et al., 1998). However, the Squamata are represented by a small number of relatively large trunk (mid-

dorsal) vertebrae and a single cervical vertebrae (**Fig 6A, B; Table 2**). Osteological nomenclature and description follows Hoffstetter and Gasc (1969) and Holmes et al. (2010).

Table 2

Measurements of greatest length (GL), anterior width (AW) and posterior width (PW) of reptile vertebrae recovered from Unit 5 at Ti's al Ghadah. All measurements are in millimetres and are taken from the dorsal surface.

Specimen	Description	GL (mm)	AW (mm)	PW (mm)
TAG14/307	mid-dorsal vertebra	13.74	13.6	13.19
TAG13/049	mid-dorsal vertebra	16.69	17.42	/
TAG13/Hc-T1	mid-dorsal vertebra	16.26	/	/
TAG14/706	cervical vertebra	12.24	9.34	6.95

Fig. 6. Reptile and bird fossils from Ti's al Ghadah. A: TAG13/049 mid-dorsal (trunk) vertebra, ventral aspect, cf. Varanidae/*Uromastyx* sp. B: TAG14/706 cervical vertebra, lateral aspect, cf. *Uromastyx*. C: TAG14/318 13th cervical vertebra, dorsal aspect, *Struthio* sp. D: TAG13/038 left tarsometatarsus, dorsal aspect, *Tachybaptus* sp. E i: TAG14/287 occipital region and base of skull of *Neophron percnopterus*, lateral aspect. E ii: TAG14/287, maxilla of *Neophron percnopterus*, lateral aspect. E iii: TAG14/269 right humerus proximal end of *Neophron percnopterus*, caudal aspect. E iv: TAG14/259 right humerus distal end of *Neophron percnopterus*, caudal aspect. F: TAG14/270 proximal end of left humerus of *Pterocles orientalis*, caudal aspect. Scale bars = 10 mm. Numbered features are referred to in the text.

4.2.1.1 Squamata

Varanidae and/or Agamidae - *Uromastyx* sp.

The centra are procoelous. The cotyles are widest dorsally with a relatively flat dorsal edge and narrow ventrally to a curved ventral margin. The condyles are orientated postero-dorsally, with a flatter ventral margin than the cotyles. The cotyles are orientated antero-ventrally and, unlike the majority of procoelous lizards, the ventral rim is retracted and exposes the entirety of ventral concave surface of the cotyle (**Fig. 6A-1**). There is no sagittal crest present on the ventral surface. These characters suggest the varanids (Varanidae) or the agamid *Uromastyx*. The cervical vertebra (TAG14/706), however, lacks a marked hypapophyseal peduncle (**Fig. 6B-2**), which suggests *Uromastyx* sp. rather than the Varanidae (Holmes et al., 2010).

4.2.2 Aves

Ten specimens are attributable to six orders, six families, seven genera and seven species (**Table 3**) and are the first Pleistocene records of birds to be reported from the Arabian Peninsula. Taxonomic conventions follow Porter and Aspinall (2010) and osteological nomenclature follows Baumel and Witmer (1993).

Table 3

Bird fossils recovered from Unit 5 at Ti's al Ghadah. GL = greatest length; Bp = proximal breadth; Sc = minimum width of shaft; Bd = distal breadth; Dp = proximal depth and Dd = distal depth. All measurements are in millimetres.

SPECIMEN	ELEMENT	side	TAXA	GL	Bp	Sc	Bd	Dp	Dd
TAG13/038	tarsometatarsus	L	*Tachybaptus* sp.	32.72	6.50	2.68	5.89	7.14	4.76
TAG14/185	humerus	L	*Anas* sp.	/	/	6.74	13.50	/	8.04
TAG14/225	femur	R	*Milvus* cf. *migrans*	/	/	6.44	13.30	/	10.07
TAG14/246	humerus	R	*Motacilla* cf. *alba*	/	6.34	/	/	/	/
TAG14/251	ulna	L	cf. *Motacilla*	/	/	/	/	/	/
TAG14/259-269	humerus	R	*Neophron percnopterus*	/	/	9.64	24.36	/	13.26
TAG14/270	humerus	L	*Pterocles orientalis*	/	16.34	/	/	10.98	/
TAG14/286	ulna	R	*Neophron percnopterus*	/	/	/	/	/	/
TAG14/287	cranium	/	*Neophron percnopterus*	/	/	/	/	/	/
TAG14/318	c. vertebra XIII	/	*Struthio* sp.	[a]	[a]	[a]	[a]	[a]	[a]

[a] **see Table 4**

459 **4.2.2.1 Struthioniformes**

460 Struthionidae

461 *Struthio* sp.

462 A thirteenth cervical vertebra (TAG14/318) is attributable to an ostrich, *Struthio* sp. (**Fig. 6C**). The
463 specimen is stained light-brown in colour with minimal weathering or abrasion. All articular surfaces
464 are well-defined, although the specimen has been crushed and is slightly compressed in the
465 dorsal/ventral direction. The facies articularis caudalis of the corpus vertebra has broken off, as have
466 the processes costalis.

467 Comparison with the type specimen for the Pleistocene taxon *Struthio asiaticus* (NHM - 23105)
468 suggests that the Nefud specimen was derived from a similarly-sized bird. The type, however, includes
469 a series of articulated cervical vertebrae that are fused in matrix to an atlas, distal tarsometatasus and
470 phalanx and this state of preservation precludes detailed morphological and metric comparison.
471 However, in terms of overall dimensions, there is no evidence to suggest an affinity with "giant"
472 Pleistocene ostrich taxa reported from the Caucuses (Burchak-Abramovich and Vekua, 1990; Vekua,
473 2013).

474 Morphological and morphometric comparisons were also conducted with specimens from
475 extant species (*S. camelus camelus*, *S. c. australis*, *S. c. massaicus* and *S. molydophanes*) and recently
476 extinct species (*S. c. syriacus*): these data are summarised in **Table 4**. TAG14/318 differs from
477 comparative specimens from the extant and recently-extinct species, *S. c. australis* and *S. c. syriacus*,
478 respectively. Viewed from the dorsal aspect, the opening to the foramen vertebra forms a much more
479 acute angle between the zygapophyses cranialis in TAG14/318 (**Fig. 6C-3**) than in the comparative
480 specimens for these taxa. The articular surfaces of zygapophyses cranialis are also much more
481 developed and robust in TAG14/318 (**Fig 6C-4**). At the caudal end, the lacuna interzygapophyses is
482 very square in TAG14/318 (**Fig. 6C-5**), as indeed are the caudal articular facets (**Fig. 6C-6**): these
483 characters are rounded in the comparative specimens. However, comparison with material from *S.*
484 *molybdophanes* (1888.5.5.1) indicates that these characters are similar. From the dorsal aspect, the
485 lacuna interzygapophyes caudalis is square and the lacuna interzygapophyses is v-shaped, rather than
486 u-shaped in *S. molybdophanes* (**Table 4**).

The Pleistocene fossil record of *Struthio* is sparse and the taxonomic and geographic affinities of Pleistocene ostriches are poorly known. As such, it is not feasible to identify this specimen beyond genus. However, it is notable that of all the compared specimens the closest match on morphological and morphometric grounds is *S. molybdophanes*, an ostrich recently promoted to full species status (Sangster et al., 2015; see also Miller et al., 2011) and currently restricted to the horn of Africa.

Table 4

Characters and measurements for specimen TAG14/318 and comparative Struthio spp. examined at NHM-Tring. Measurements: GL = greatest length; B cran = cranial breath; B caud = caudal breadth; H cran = cranial height. All measurements were taken from the dorsal surface and are in millimetres.

		CHARACTERS			MEASUREMENTS				
Specimen	**Taxon**	**1**	**2**	**3**	**GL (dor)**	**B cran**	**B caud**	**H cran**	**notes**
TAG14/318	*Struthio* sp.	v-shaped	square	flat	71.96	38.64	38.73	(27.96)	crushed d/v
1857.2.24.10	*S. c. australis*	u-shaped	round	rounded	73.61	40.7	42.16	32.12	female
1888.3.5.1	*S. molybdophanes*	v-shaped	square	flat	70.4	40.05	43.02	28.42	Somlalia
1846.10.17.7	*S. c. camelus*	u-shaped	round	rounded	77.24	42.43	44.05	35.52	male - Gambia
1915.3.30.1	*S. c. massaicus*	inter.	round	flat	71.7	35.42	37.12	29.98	male
S.1972.1.2	*S. camelus*	inter.	round	rounded	75.48	42.02	44.96	29.96	female - captive
S.1954.5.1	*S. camelus*	u-shaped	round	rounded	70.84	36.91	40.79	31.16	female - captive
1923.6.10.1	*S. c. syriacus*	u-shaped	square	rounded	61.42	31.96	38.32	24.36	extinct
1924.4.81	*S. c. syriacus*	u-shaped	square	rounded	62.06	36.24	40.08	27.64	extinct

1 – shape of foramen vertebra; 2- shape of lacuna interzygapophyses 3 – shape of caudal articular facets.

4.2.2.2 Podicipediformes

Podicipedidae

Tachybaptus sp.

A well-preserved, complete left tarsometatarus (**Fig. 6D**) first reported in Stimpson et al. (2015) is derived from a small grebe of the genus *Tachybaptus*, which contains one species, *T. ruficollis*. The specimen is an excellent match for the genus. At the distal end of the element, the end of the lateral edge of the trochlea metatarsi II curves to the diaphysis and the lateral side of the trochlea metatarsi IV is flat. At the proximal end, the hypotarsus is equal height to the condylus interarticularis (cf. Fjeldså, 2004, 214).

TAG13/038 is notably shorter overall (**Fig. 7A**), but is not less robust than the comparative material at NHM-Tring. To date, morphological and metric comparisons have been limited to comparative material of European provenance (**Table S3 supplementary data**) and extant Oriental subspecies are "generally smaller" than their counterparts from higher latitudes (Fjeldså, 2004, 153). There are differences, however, between the relative positions of the medial trochlea (**Fig 6D-7**) and foramen vasculare distale (**Fig. 6D-8**) in the TAG specimen and the comparatives. We withhold a specific attribution until it can be determined if this variation falls within specific limits for *T. ruficollis* or represents a novel Pleistocene form.

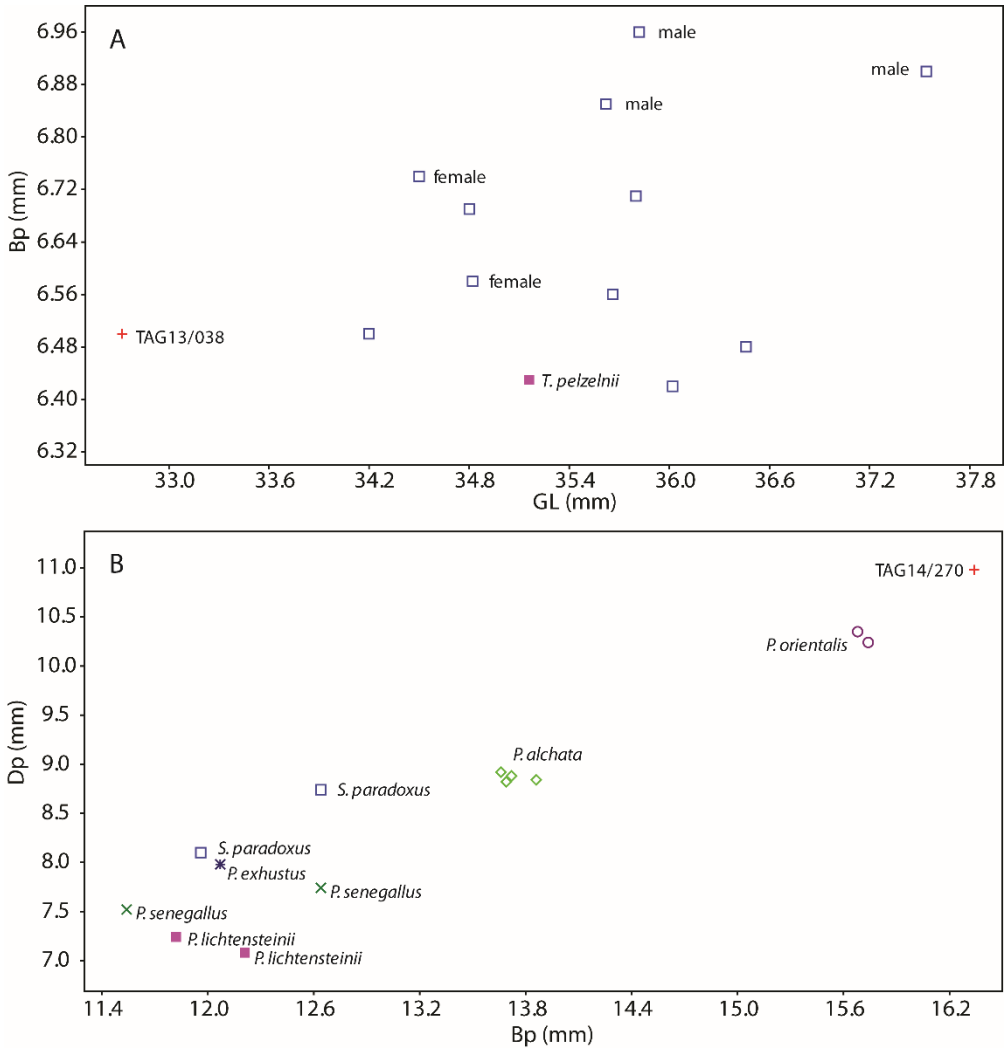

Fig. 7. Bivariate plots to show A: measurements of tarsometatarsus TAG13/038, *Tachybaptus* sp., with comparative specimens of *T. ruficollis* (open square) and *T. pelzelnii* (closed square) at NHM-Tring. GL = greatest length; Bp = proximal breadth. B: measurements of the proximal humerus TAG14/270, *Pterocles orientalis* with comparative specimens of *Pterocles* spp. and *Syrrhaptes* sp. Bp = proximal breadth; Dp = proximal depth.

520

521 **4.2.2.3 Accipitriformes**

522 Accipitridae

523 *Neophron percnopterus*

524 The mineralised remains of a cranium (TAG14/287- **Fig. 6E i and ii**), a complete right humerus
525 (recovered in two pieces, TAG14/259 and 269**; Fig. 6E iii and iv**) and a complete, but very friable right
526 ulna (TAG14/286) were found in close proximity in trench one and are clearly attributable to Egyptian
527 vulture, *Neophron percnopterus* (cf. NHM 1847.10.21.25). These specimens are a relatively early
528 record of this species, which is present in the Ti's al Ghadah area today (CMS, personal observation).

529 The remains of the cranium consist of the occipital region and cranial vault (**Fig.6E i**). A semi-
530 circular puncture (maximum dimensions = 11.60 mm × 8.78 mm) is evident to the right side of the
531 vault, which we interpret as a tooth mark (**Fig. 6E i-9**). There may also be a second puncture just above
532 the foramen magnum although this may be a break associated with weakening of the bone around the
533 edge of the foramen. The maxilla is also present and is complete from os nasale to rostrum maxillare
534 (**Fig. 6E ii**). The humerus is complete though was recovered in two pieces (**Fig 6E iii and iv**). There is
535 extensive evidence of gnawing/chewing on the caudal and cranial surfaces. The crista deltopectoralis
536 appears gnawed along much of the dorsal edge (**Fig. 6E iii-10**) and there are multiple small (maximum
537 dimensions: 2.5 × 2.5 mm) pits in the cranial surface of the distal end of the element (**Fig. 6E iv-11**).
538 The ulna is complete, but friable. It was recovered much closer to the section edge and is likely to have
539 been re-exposed and weathered. The ulna has also been chewed, apparently by a small to medium-sized
540 carnivore.

541

542 *Milvus* sp. (cf. *migrans*)

543 A fragment of a distal end of a right femur (TAG14/225) indicates the presence of a kite. While it is
544 notoriously difficult to separate skeletal elements of the genus *Milvus* sp. (e.g. Morales Muniz, 1993),
545 the relatively small size of the specimen and comparison with the specimens at Tring is suggestive of
546 black kite (*Milvus migrans*).

547

548 **4.2.2.4 Pteroclidiformes**

549 Pteroclididae

550 *Pterocles orientalis*

551 TAG14/270 is a fragment of a left proximal humerus from a large sandgrouse species (**Fig. 6F**). While
552 it is a reasonable morphological match for *Syrrhaptes* sp., TAG14/270 is markedly larger and more
553 robust: the caput humeri (**Fig. 6F-12**) is more developed and more prominent as in *Pterocles* sp. It can
554 be difficult to separate the skeletal elements of different *Pterocles* species (e.g. Dobney et al., 1999) but
555 TAG14/270 is clearly from a large bird (**Fig. 7B; Table S4 supplementary data**) and all observable
556 characteristics match those of *P. orientalis*.

557

558 **4.2.2.5 Anseriformes**

559 Anatidae

560 *Anas* sp.

561 Two fragments of the distal end of a left humerus (TAG14/285) is from a dabbling duck of the genus
562 *Anas*. It is not possible to identify this specimen to species, but it derived from a bird equivalent in size
563 to a mallard (*Anas platyrhynchous*).

564

565 **4.2.2.6 Passeriformes**

566 Motacillidae

567 *Motacilla* cf. *alba*

568 Two small, mineralised and well preserved specimens - a fragment of a right proximal humerus
569 (TAG14/246) and a left ulna (TAG14/251) - are derived from passerines. Comparisons under a lower
570 power microscope with the comparative collections at NHM-Tring indicate that they are both
571 attributable to the genus *Motacilla* (wagtails), most likely *M. alba*.

572

573 **4.2.3 Mammalia**

574

575 **4.2.3.1 Carnivora**

Felidae

Panthera

A total of four specimens known from Ti's al Ghadah are attributable to the genus *Panthera* (**Table 5**). Two of these, a left third metacarpal (JMI 27) and a right fourth metacarpal (TAG13/097), have been referred to the extinct Eurasian jaguar, *Panthera (onca) gombaszogensis* (see Thomas et al., 1998 and Stimpson et al., 2015, respectively). Morphological and morphometric analyses of TAG13/097 are described in Stimpson et al. (2015). While comparative sample sizes are small, measurements for JMI 27 appear equivalent with published measurements for Pleistocene jaguars, *P. onca augusta* and *P. onca gombaszogensis* (**Table S5, Fig. S2 supplementary data**). The genus is also represented by a phalanx (TAG14/339) and broken mandibular canine (TAG13/145) (**Fig. 8A, B**).

Table 5

Carnivora measurements from Unit 5 at Ti's al Ghadah. Measurements: GL = greatest length; Bp = proximal breadth; Dp = proximal depth; MDAP = minimum antero-posterior diameter of diaphysis; MWML = minimum medio-lateral width of diaphysis; Bd = distal breadth; Dd = distal breadth; M-D = mesio-distal length; B-L = buccal-lingual width; HFM = height of foramen magnum; WFM = width of foramen magnum; WOC = width across occipital condyles; BJP = breath across jugal processes; Ltald = length of talonid. All measurements are in millimetres.

Specimen	Element	Taxon	Measuements	Source
JMI 27	left metacarpal III	*Panthera* cf. *gombaszogensis*	GL = 91.94; Bp = 22.16; Dp = 20.70; MDAP = 11.74; MWML = 12.05; Bd = 20.75; Dd = 18.21	Thomas et al. (1998); metrics: this study
TAG13/097	right metacarpal IV	*Panthera* cf. *gombaszogensis*	GL = 88.72; Bp = 17.16; Dp = 19.14; MDAP = 11.74; MWML = 11.40; Bd = 17.30; Dd = 18.04	Stimpson et al. (2015)
TAG13/145	mandibular canine	*Panthera* sp.	M-D = > 17.00; B-L = 13.22	this study
TAG14/339	phalanx I	*Panthera* sp.	GL = 48.70; Bp = 19.20; Dp = 14.91	this study
TAG14/245	occiptal	*Canis sp.*	HFM = 16.1; WFM = 18.30; WOC = 30.77; BJP = 42.58	this study
TAG14/184	M_1 (carnassial)	*Canis anthus*	M-D = 21.20; B-L = 8.04; Ltald = 6.22	this study

Hyaenidae

cf. *Crocuta crocuta*

A total of seven coprolites were during the excavations: six specimens from trench 1 and a one specimen from trench 6. The general morphology of intact specimens - a near circular cross-section, with convex and concave ends - closely resembles hyeana, most likely *Crocuta crocuta* (Larkin pers comm.; Parfitt pers. comm). Measurements (following Larkin et al., 2000) of one complete specimen, TAG14/256 (**Fig. 8C**: axial length 40.58 mm; diameter A 29.85 mm, diameter B 28.43 mm) fall within reported ranges of coprolites from this taxon (cf. Larkin et al., 2000; Lewis et al., 2010).

Canidae

Canis sp.

A fragment of the base of the skull (TAG14/245), a lower right carnassial (TAG14/184) and a fragment of a lumbar vertebra (TAG14/208) are attributable to a medium-sized canid. The skull fragment consists of the occipital region and a fragment of the supra-occipital (**Fig. 8D**). The foramen magnum, occipital condyles and condylar foramen are intact and portions of the par-occipital process and basi-occipital are present. This specimen is a good morphological match with comparative material for the golden jackal, *Canis aureus*: measurements indicate that it derived from a relatively large individual (**Table 5**).

Fig. 8. Carnivora fossils from Ti's al Ghadah A: TAG14/339 phalanx, volar and plantar aspects, *Panthera* sp. B: TAG13/145 broken mandibular canine, *Panthera* sp. C: TAG14/256 coprolite, cf. *Crocuta crocuta*. D:

TAG14/245, occipital region, caudal aspect, *Canis* sp. E: TAG14/184, right M_1 (carnassial), *Canis anthus*, buccal (i) and lingual (ii) aspects. Scale bars = 10 mm. Numbered features are referred to in the text.

Canis anthus (syn. *Canis aureus* [*lupaster*]; *Canis lupus lupaster*)

TAG14/184 is a trenchant, lower right carnassial (M_1). With the exception of the break to the mesial root, the specimen is complete and is relatively unworn **(Fig. 8E)**. The specimen, however, appears iron-stained and there is marked "sidedness" in weathering: it appears that the tooth ultimately lay on its buccal side prior to burial as there is minimal modification to this surface of the tooth (**Fig. 8E i**). Conversely, the lingual side is abraded across the entire surface (**Fig. 8E ii**).

TAG14/184 is too large to have derived from any known *Vulpes* sp. and is from a medium-sized canid (**Table 5**). The carnassial is trenchant, with a sub-equal bicuspid talonid (**Fig. 8E ii-1**) and a relatively well-developed metaconid (**Fig. 8E ii-2**). The hypoconid is not centrally-located and is angular rather than conical. These characters indicate *Canis* sp. and discount the hypercarnivorous *Cuon* and *Lycaon* (cf. Baryshnikov and Tsoukala, 2010; Baryshnikov, 2012; Brugal and Boudadi-Maligne, 2011; Petrucci et al., 2012)

The morphometric characteristics of TAG14/184 indicate that it derived from a smaller animal than Pleistocene and recent records of European and regional *C. lupus lupus* (cf. Flower and Shreve, 2014; Sansalone et al., 2015), recent records of *C. lupus pallipes* (cf. Dayan, 1994) and Pleistocene and recent records of *C. lupus arabs* from the Levant (**Fig. 9**). Conversely, measurements from TAG14/184 suggest that it derived from an animal that is larger than recent European jackals, recent and Pleistocene African jackals (*C. aureus* s.s) and match equivalent measurements of a large form of jackal, variously classified as *Canis aureus lupaster* or *Canis lupus lupaster* (**Fig. 9**).

Osteological studies have long recognised the likelihood of a large extant form of jackal in North Africa (Huxley, 1880) and "large" jackal fossils (classified as *Canis aureus*) are known from Middle to Late Pleistocene in Northwest Africa (Geraads, 2011). Recent work with mitochrondrial and nuclear genome data, however, has indicated that these North African "jackals" are a cryptic species more closely related to grey wolves (*C. lupus*) and occupy a much wider geographical area and range

of habitats in Africa than was previously thought (Rueness et al., 2011; Gaubert et al., 2012; Koepfli et al., 2015). The trenchant morphology and morphometric characteristics of TAG14/184 are a close match for these "large forms" and we follow Koepfli et al. (2015) and refer this specimen to *Canis anthus*, the African golden wolf.

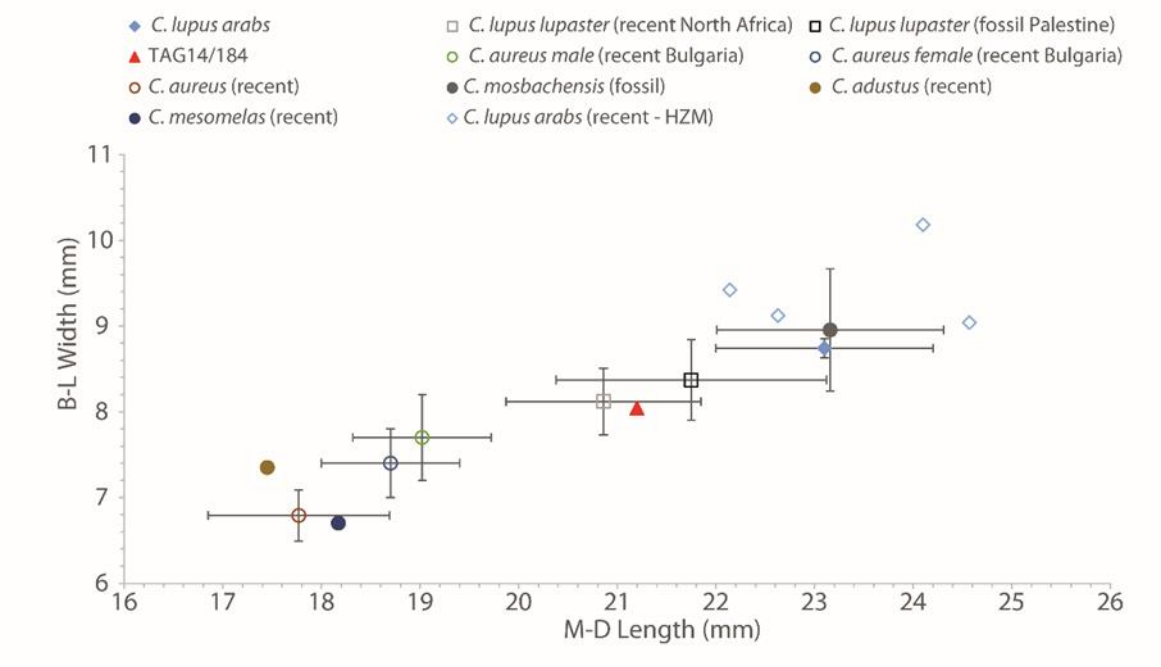

Fig. 9. Bivariate plot to show mean values, ranges (1 sigma) and single observations of length (M-D = mesio-distal) and width (B-L = buccal-lingual) measurements for lower carnassial teeth (M_1) from recent and fossil *Canis* sp. with fossil specimen TAG14/184. Data compiled from Kurten, 1965; Dayan et al., 1992; Dayan, 1994; Rook and Azzaroli Puccetti, 1996; Baryshnikov, 2012; Stoyanov, 2012; Measurements of recent *C. lupus arabs* were also taken from comparative specimens at the HZM.

Vulpes sp.

Thomas et al. (1998) reported the presence of the bones of foxes with no discernible morphological differences from extant *Vulpes vulpes*. Small cranial fragments were recovered in 2013 (Stimpson et al., 2015), but no further specimens have yet been identified in Unit 5.

cf. Mustelidae

A single left mandibular canine (antero-posterior length = 3.56 mm; buccal-lingual width = 2.34 mm) with a marked cingulum on the medial side of the tooth is most likely attributable to the Mustelidae. Measurements suggest that it derived from an animal similar in size to a large *Mustela* sp. or *Vormela* sp. but further comparative material is required.

4.2.3.2 Perissodactyla

Equidae

In addition to small numbers of rib fragments and a thoracic vertebrae, three well preserved specimens attributable to the Equidae were recovered (**Table 6**): a fragment of a right mandible (TAG14/329; **Fig. 10A, B**), a complete left astragalus (TAG14/342; **Fig. 10C**) and a near-complete left femur (TAG13/146; **Fig. 10D**).

Table 6

Measurements of fossils of the Equidae from Ti's al Ghadah. Abbreviations: TAG14/329 - MD = mesial-distal length; BL = buccal-lingual width; Lo = length of occlusal surface; lo = width of occlusal surface; LDB = length of double knot. TAG13/146 – GL = greatest length; mL = medial length; Bp = proximal breadth; Sc = minimum width of diaphysis; Bd = distal breadth; Dd = distal depth. TAG14/342 - astragalus measurements follow the locations and conventions described in Alberdi and Palombo (2013). All measurements are in millimetres.

Specimen	**Element**		**MD**	**BL**	**Lo**	**lo**	**LDB**
TAG14/329	right mandible	M_3	(c.33.85)	15.98	(c. 32)	13.2	14.81
		M_2	25.6	18.88	25.08	14.18	15.31
Specimen	**Element**	**GL**	**mL**	**Bp**	**Sc**	**Bd**	**Dd**
TAG13/146	left femur	c. 350	306	c. 114.66	43.77	96.68	c. 100
Specimen	**Element**	**1**	**2**	**4**	**5**	**6**	**7**
TAG14/342	left astragalus	65.16	66.5	67.91	56.16	37.9	57.65

The Pleistocene equids of the Middle East are generally thought to comprise of *E. caballus*, *E. hydruntinus* and *E. hemionus* (Eisenmann et al., 2002). The separation of different equids on the basis of dental morphology, however, is not a straightforward issue. Morphological criteria can be unequivocal (e.g. Azzaroli and Stanyon, 1991; Giegl and Grange, 2012) and the nomenclature employed in schemes varies between authorities. For TAG14/329, we follow criteria described in Davis

(1980), Eisenmann et al. (2008), van Asperen et al. (2012), Geigl and Grange (2012) and Alberdi and Palombo (2013).

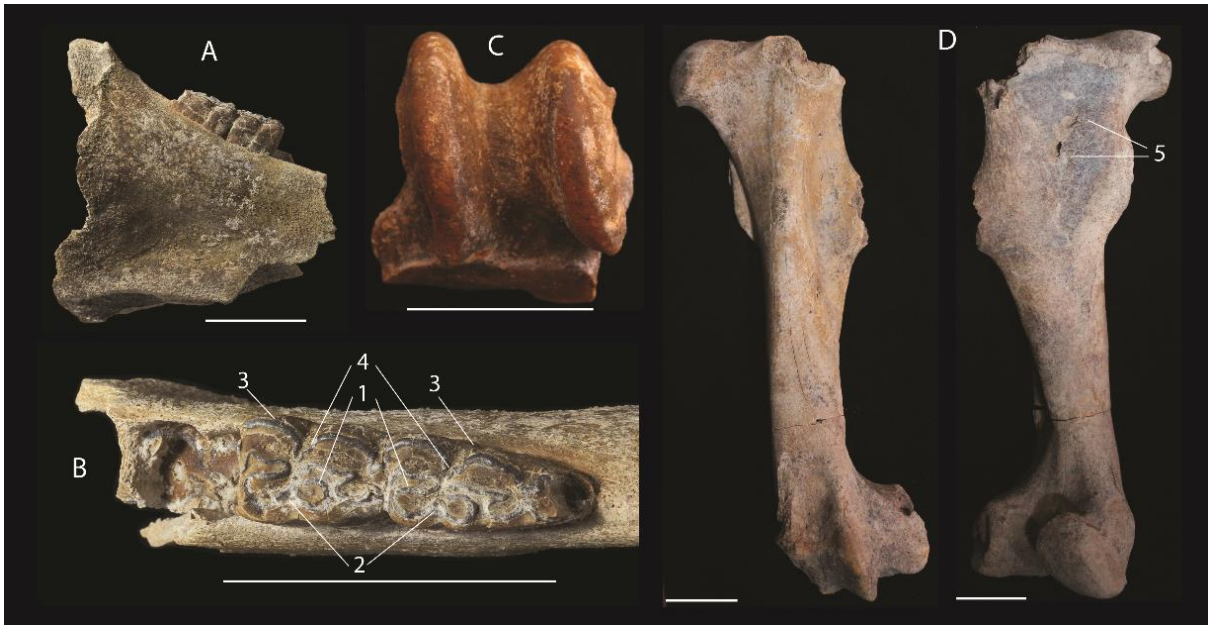

Fig. 10. Fossils of Equidae from Ti's al Ghadah. TAG14/329 right mandible, *Equus hemionus*, in A: lateral and B: occlusal views. C: TAG14/342 left astragalus, *Equus* sp., dorsal aspect. D: TAG13/146 left femur, *Equus* sp., cranial and caudal views. Scale bars = 50 mm. Numbered features are referred to in the text.

Equus hemionus

TAG14/329 is a fragment of a robust right mandible (**Fig. 10A**). The first molar is broken off at the root below the alveolus, but the worn second and third molars are in situ. The M_2 is intact. The M_3 is largely complete but is there is a break to the distal occlusal surface (**Fig. 10B**). Caballoid horses can be discounted as the double knots on M_2 and M_3 are rounded (**Fig. 10B-1**) with v-shaped (rather than u-shaped) lingual valleys (linguaflexids; **Fig. 10B-2**) and rounded (rather than flat) buccal margins of the protoconid and hypoconid (**Fig. 10B-3**), although this last characteristic is regarded as an unreliable means to discriminate between taxa (Davis, 1980). While tooth wear is marked, the vestibular grooves (ectoflexids) on each molar appear shallow and they do not penetrate the isthmus of the double-knot (**Fig. 10B-4**). This would discounts zebras and zebra-like taxa, the extinct *E. hydruntinus* and Pleistocene stenonine horses and indicate the hemione, *E. hemionus*. Morphometric comparisons using the intact M_2 of TAG14/329 suggest the dimensions of the occlusal surface are larger than equivalent

703 data from extant and recently extinct regional sub-species (*E. h. onager* and *E. h. hemippus*,
704 respectively) and equivalent to extant Mongolian subspecies *E. h. hemionus* and the Tibetan species, *E.*
705 *kiang* (**Fig. 11**).

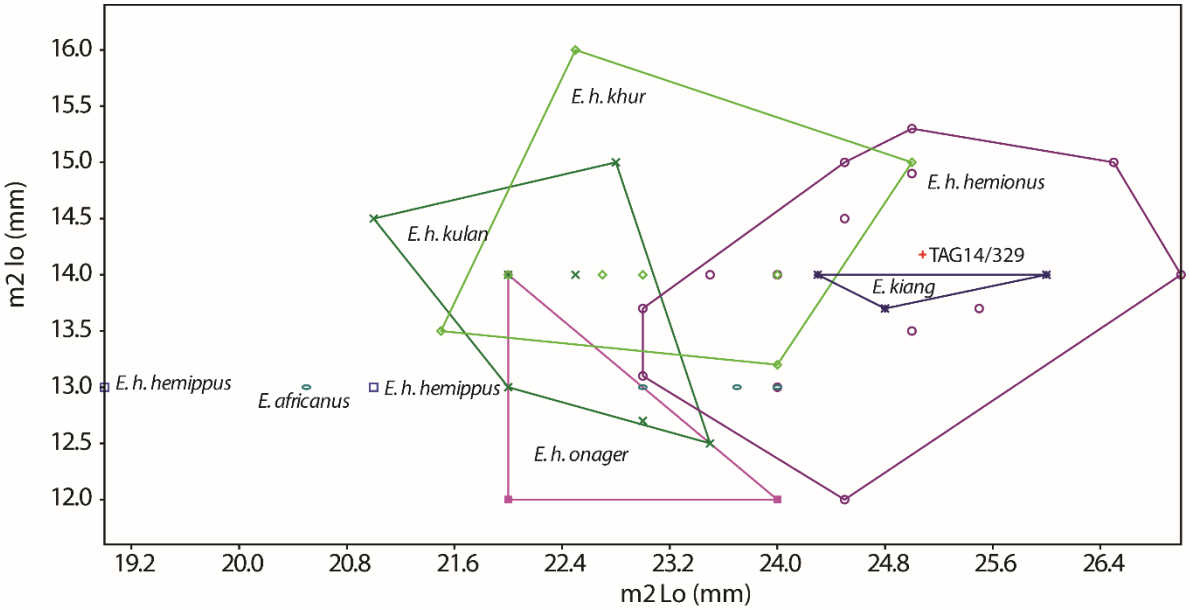

706

707 **Fig. 11.** Bivariate plot to show length of occlusal surface (Lo) and width of occlusal surface (lo) of second lower
708 molars (M_2) for five subspecies of *Equus hemionus*, *E. kiang* and *E. africanus* with fossil specimen TAG14/329.
709 Comparative data compiled from http://www.vera-eisenmann.com/. Convex hulls fitted in PAST (Hammer et
710 al., 2001).

711 *Equus* sp.

712 In terms of the small sample of post-crania, the specimens are rather robust. The dimensions of a near-
713 complete left femur TAG13/146 (**Table 6; Fig. 10D**), notable for the presence of carnivore pits on the
714 caudal surface, near to the proximal end (**Fig. 10D-5**), indicate that this specimen is large and robust in
715 comparison to extant hemiones (**Fig. 12A).** The dimensions of a complete left astragalus (TAG14/342;
716 **Fig. 10C**), which was found in close association with mandible TAG14/329, are also large and robust
717 in comparison to extant hemiones (**Fig. 12B**). We cannot assume, however, that the two specimens
718 derived from the same individual and a PCA analyses of six variables (**Table 6**) suggests that is also of
719 a size and proportion of larger equid taxa than the extant hemiones, equivalent perhaps to *Equus*
720 *oldowayensis* (**Fig. 12B**). This would be consistent with the findings reported in Thomas et al. (1998)

who also describe relatively large and robust bones from the site, possibly from a robust stenonid horse or species of zebra.

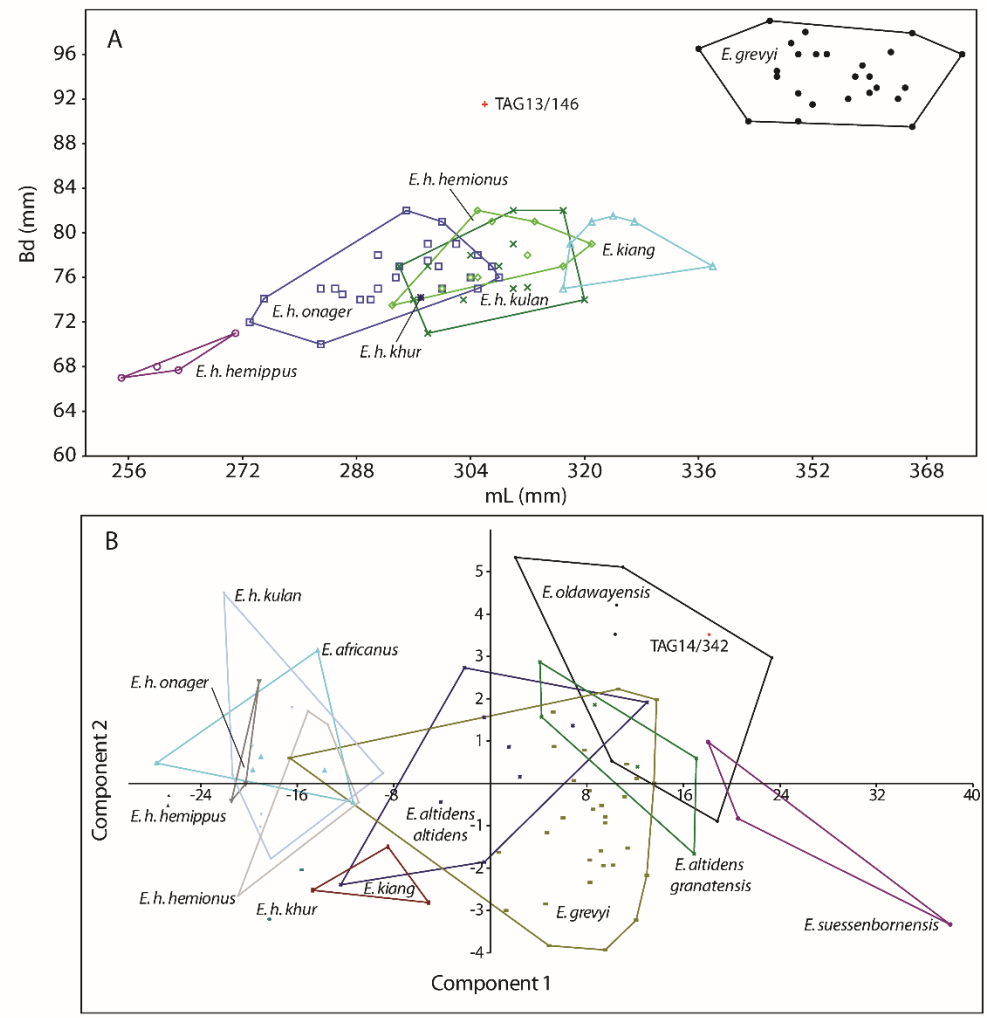

Fig. 12. A: Bivariate plot to show medial length (mm) and distal breath measurements of fossil femur TAG13/146 with comparative data from five sub-species of *E. hemionus*, *E. kiang* and *E. gevyi*. Comparative data compiled from http://www.vera-eisenmann.com/. Convex hulls fitted in PAST (Hammer et al., 2001). B: Principal components analysis scatter for six metric variables of fossil astragalus TAG14/342 and comparative data from extant and extinct *Equus* spp. Data compiled from http://www.vera-eisenmann.com/, Alberdi and Palombo (2013) and comparative specimens at NHM-SK.

Given that Eisenmann et al. (2008) report that the various subspecies of *E. hemionus*, as they are known from the fossil record, appear to have been conservative in terms of overall dimensions and proportions there are two possible scenarios for the interpretation of the equid remains in hand. Firstly,

734 that there are the remains of more species of equid preserved at the site than the available dental material
735 indicates, or secondly that the equid remains at Ti's al Ghadah represent a large and robust Pleistocene
736 form of *E. hemionus*.
737
738 **4.2.3.3 Proboscidea**
739 The presence of bones from a large elephant was identified in 2013, with a 2.25 m long tusk
740 (TAG13/052) and right magnum (carpal III - TAG13/104) recovered. Stimpson et al. (2015) tentatively
741 proposed that these remains were attributable to the extinct genus *Palaeoloxodon* (sometimes classified
742 as *Elephas*). In 2014, collaborative investigations of the elephant remains of Ti's al Ghadah began
743 between the SCTH, SGS and Palaeodeserts project, with the establishment of large-scale investigations
744 by the SGS at the south of the ridge (**Fig. 3; Fig. 5A**). Here, we focus on the taxonomic diagnosis of
745 two diagnostic specimens, an upper molar TAG14/301 (**Fig. 13A, B**) and a mandible of a young animal,
746 TAG14/281 (**Fig. 13C, D**).
747
748 **Elephantidae**
749 *Palaeoloxodon* cf. *recki*
750 The lineage of the straight-tusked elephant is generally included within *Elephas* Linnaeus, 1758 by
751 workers on African material (e.g. Sanders et al., 2010) but *Palaeoloxodon* Matsumoto 1924 or *Elephas*
752 (*Palaeoloxodon*) by those studying Eurasian remains (e.g. Palombo and Ferretti 2005; Lister, 2016).
753 Pending resolution of the relationships among elephant genera we here retain the genus *Palaeoloxodon*
754 for clarity (cf. Shoshani and Tassy 1996).
755 Specimen TAG14/301 is a portion of an adult left upper molar in mid-wear (**Fig. 13A**). The
756 anterior end of the crown shows signs of both natural (lifetime) wear and post-mortem breakage; at the
757 posterior end lamellae have been lost post-mortem. Specimen TAG14/281 is a portion of a juvenile
758 mandible including a complete molar in early to mid-wear.

Fig. 13. Elephantidae fossils from Ti's al Ghadah. TAG14/301, upper left molar, *Palaeoloxodon*, in A: occlusal view and B: lateral view. TAG14/281, right mandible in C: occlusal view, and D: lateral view. Scale bars = 100 mm.

The molars show features which strongly suggest referral to the genus *Palaeoloxodon*. In particular, the occlusal wear figures show lamellae with distinctly but roughly folded enamel, and irregular expansions at roughly the mid-line of the molar, extending in both the anterior and posterior directions from the anterior and posterior enamel bands, respectively. These features are distinctive of *Palaeoloxodon* and distinguish these molars from other candidate genera, *Loxodonta* (African elephants), *Mammuthus* (mammoths) and *Elephas* s.s. (lineage of Asian elephant). Another common feature of *Palaeoloxodon*, rings of enamel medial and lateral to each lamella in early wear, are not visible these specimens; this character is not, however, invariably present in the genus.

Upper molar TAG14/301 preserves 11 enamel lamellae, but this is incomplete and the original number (and the original length of the tooth) are difficult to reconstruct. At the anterior end, the preserved crown is worn to the root at the front, and the isolated 'anterior root' has been lost through wear, so it is not possible to reconstruct the number of lamellae lost (Lister and Sher, 2015; Sher and Garutt, 1987). The base of a somewhat isolated root is visible at the antero-lateral corner of the crown,

but it is not of the correct shape or position to be the true 'anterior root' and must therefore be one of the 'paired roots' behind it. It is therefore likely that at least 2-3 lamellae have been lost through wear, but the precise number is unknown.

Loss at the posterior end is also difficult to quantify. The large size of the molar makes it very likely to be either M^2 (the penultimate of the series) or M^3 (the last of the series). In a more complete specimen, this can easily be determined from the shape of the posterior end of the crown, which tapers in M^3 but is blunt and wide in M^2. Unfortunately, breakage makes the determination of this characteristic is problematic for TAG14/301. The width of the crown reduces very slightly from front to back (**Table 7**), which might suggest M^3, but this is insufficient for certainty. A second factor is crown height, which tends to be maximal near the front of the molar in M^3 and near the back in M^2. However, because only the posterior two preserved lamellae of this specimen are unworn and allow measurement of crown height, this cannot be determined. The crown is relatively high (133 mm, for a molar width of 90.5 mm, giving a preserved hypsodonty index of 100 x 133/90.5 = 147), which would be consistent with either a lamella close to the original posterior end of an M^2, or a lamella half to two-thirds down the crown of an M^3. The remaining exterior surface of the molar near the posterior break provides some evidence: especially near the top of the crown on the lateral side it curves medially to a degree that suggests it is close to the natural posterior end of the tooth, rather than that the tooth extended much beyond the break. In this case, the molar would be an M^2, but this cannot be considered certain. If it is an M^2, then the curvature of the surface suggests that approximately two lamellae (plus the posterior talon) should be added to the preserved number. That would give an approximate total of at least 15 (two or more at the front, two at the back, and 11 preserved). If, however, the molar is an M^3, then an unknown number is missing at the back and the total is known only to be greater than 15. **Table 7** shows measurements for the Ti's al Ghadah teeth, in comparison with published data for *P. antiquus* and *P. recki recki*, the latest chrono-subspecies, with a chronological range in East Africa of ca. 1.2 – 0.5 Ma.

Table 7

Measurements of Ti's al Ghadah elephant molars compared to East African *P. recki recki* and European *P. antiquus*. Comparative data for *P. r. recki* compiled from Beden (1979), Ferretti et al., (2003), Saegusa and Gilbert

(2008), and for *P. antiquus* from unpublished data of AML and P. Davies. Measurements are in millimetres and are shown as ranges for samples where $n \leq 5$, and mean ± standard deviation for samples where $n > 5$.

	Width	Length	Plate number	Lamellar Frequency	Enamel Thickness	Hypsodonty Index
$M^{2/3}$TAG 14/301	**90.5**	**>171**	**≥15**	**6.40**	**2.7**	**≥147**
M^2 *P. recki recki*	65-80	250	10	5.0-6.8	2.0-2.5	198
M^3 *P. recki recki*	89.2 ± 7.6	315-360	13-19	5.82 ± 0.74	2.73 ± 0.29	180 ± 16
M^2 *P. antiquus*	74.1 ± 7.99	200 ± 33	11.7 ± 1.0	6.57 ± 0.99	2.33 ± 0.38	221 ± 34
M^3 *P. antiquus*	83.4 ± 6.89	284 ± 40	17.3 ± 1.5	6.18 ± 0.82	2.68 ± 0.51	213 ± 16
dP_4 TAG 14/281	**[≥44]**	**128**	**10**	**9.13**	**1.3**	**ca. 130**
dP_4 *P. recki recki*	- (dP^4=55)	- (dP^4=89)	- (dP^4=8)	- (dP^4=7.7-8.9)	- (dP^4=1.3-1.7)	- (dP^4=130)
dP_4 *P. antiquus*	47.3 ±6.5	98-145	9-11	8.92 ± 1.43	1.50 ± 0.31	164 ± 3.4

The measurement data tend to identify the upper molar TAG14/301 as an M^3 rather than M^2. If we are correct that at least two lamellae are missing from each of its anterior and posterior ends, so that its original value was at least 15, this places it in M^3 range. M^2 of *P. recki recki* is represented by only one specimen, with 10 plates, but the range probably extended to 12 as this value is found even in earlier samples referred to *P. recki ileretensis* and *P. recki atavus* (Beden, 1979). However, 15 plates have not been recorded in any M^2 of *P. recki* and even in the more advanced *P. antiquus* of Europe: 11-14 is typical for M^2 (and 16-19 in M^3). The rather thick enamel of TAG14/301 also supports identification as M^3, although this is less secure. Following Laws (1966) scheme, TAG14/301, if it is an M^3 as here suggested, is probably around wear stage XXII-XXIII, suggesting an age of roughly 40 years.

The juvenile mandible TAG 14/281 preserves dP_4 complete: its lamellar formula is x10x (10 lamellae plus anterior and posterior talons). Its crown is part-buried in the jaw, but from a micro-CT scan its crown height is ca. 57 mm and width 44 mm, giving a hypsodonty index of ca. 130. Mesowear angles were measured on the M^3 and dP_4 following Saarinen et al. (2015). The angles are measured between the ridges of enamel bounding each lamella, and the floor of dentine inside. Averaged over several lamellae the angles are 120° for the M^3 and 136° for the dP_4. The dP_4 in TAG14/281 is in early to mid-wear and at wear stage V in Laws (1966) scheme, which corresponds to an age at death of approximately 3 years.

825 Having established the generic attribution and the likely position of the teeth in the tooth-row,
826 the question of species attribution can be considered. *Palaeoloxodon* from Africa are generally
827 identified as *P. recki*; those from mainland Europe as *P. antiquus*. Remains from the Levant have
828 generally been equated with *P. antiquus* but Saegusa and Gilbert (2008) identified *P. recki* among the
829 earliest (ca. 800 ka) records. The identity of remains from the Arabian Peninsula therefore cannot be
830 assumed, and the situation is further complicated by the evolving molar morphology of *P. recki* through
831 its 3 million year history, with increasing plate number and crown height (Beden, 1979; Todd, 2001;
832 Lister, 2013). However, given the independent evidence for a Middle Pleistocene age of the Ti's al
833 Ghadah assemblage (section 4.3), we restrict our comparisons to the latest subspecies, *P. recki recki*,
834 with a known duration of ca. 1.5 – 0.4 Ma or possibly a little younger (Sanders et al., 2010). We
835 provisionally exclude its Middle to Late Pleistocene descendent *P. iolensis* of North Africa, as its molar
836 morphology shows derived characteristics not shared with *P. recki* or the Ti's al Ghadah molars.
837 Insufficient comparative work has been done between the molars of *P. recki recki* and *P.*
838 *antiquus*. However, in terms of occlusal morphology, the two molars available from Ti's al Ghadah
839 can be closely matched with available specimens of both taxa (see, for example, illustrations of *P. recki*
840 *recki* in Beden (1979), and of *P. antiquus* in Guenther (1977)). Similarly, the measurements that could
841 be taken on these specimens are within the known ranges of both species (Table 7). The taxa are
842 potentially separable on plate number and hypsodonty index of complete third molars, where their
843 ranges overlap but the variation in both variables extends to lower values in *P. r. recki* and to higher
844 values in *P. antiquus*. The recovery of further dental remains of elephant from Ti's al Ghadah may
845 therefore allow a clearer taxonomic designation in the future. For the present, we follow precedent in
846 referring them to *Palaeoloxodon* cf. *recki* in view of their more likely geographical origin from African
847 populations than European.
848
849 **4.2.3.4 Bovidae**
850 Hippotraginae
851 *Oryx* sp.

852 The vertebrate remains from Unit 5 were numerically dominated by elements from the Bovidae (**Fig.**
853 **5A**), although it is not a diverse assemblage: all examined cranial and dental remains, and identifiable
854 post-crania were attributable to the genus *Oryx*. While NISP (number of identified specimens) counts
855 were relatively high compared to other taxa, estimates of minimum numbers of individuals (MNI)
856 compiled for trenches 1 and 2 and 5 and 6, indicated a MNI of 5 (five left mandibles) and 6 (six right
857 metatarsals), respectively and suggest that a relatively low number of individuals were represented.
858 Specimens were rarely encountered in strict anatomical position (occasional cervical vertebrae) but it
859 was clear that multiple skeletal elements from single individuals were recovered in close proximity.
860 The entire skeleton was represented, although the assemblages were characterised by a relative low
861 abundance of specimens from the proximal axial skeleton (humerus and femur; **Fig. 14**).

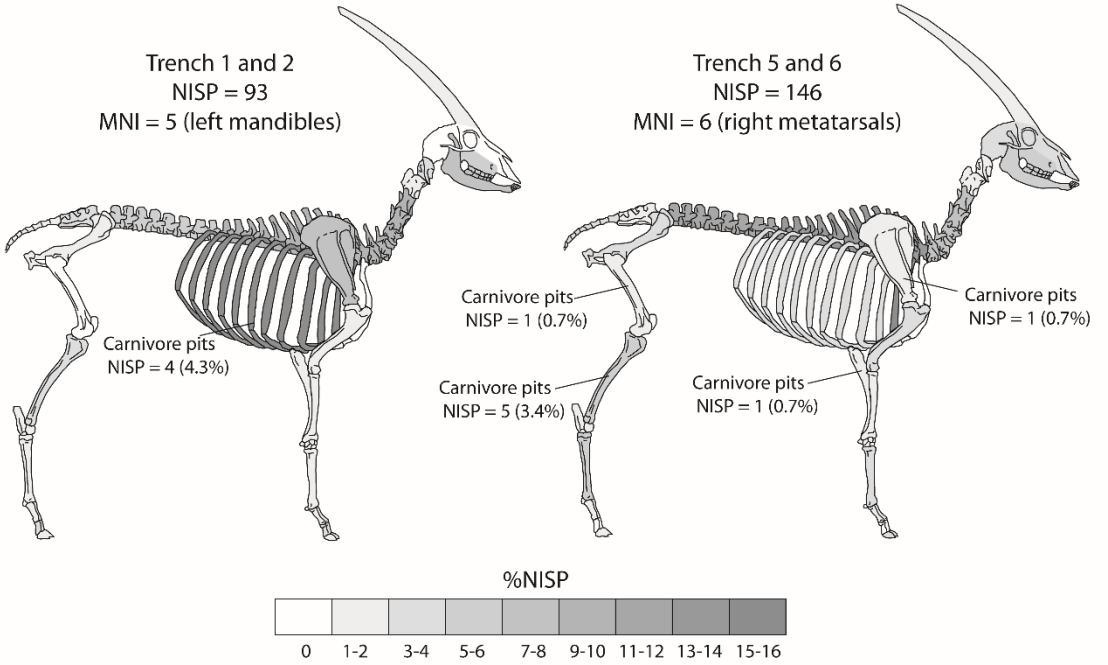

862

863 **Fig. 14.** Skeletal element representation of *Oryx* sp. expressed as % Number of Identified Specimens (NISP),
864 with estimates of Minimum Number of Individuals (MNI) and location of carnivore pits, compiled from
865 trenches 1 and 2 and trenches 5 and 6 at Ti's al Ghadah.

866

867 A number of factors can mediate attrition in different portions of the skeleton and the analysis
868 of skeletal element representation is not a straightforward issue (e.g. Marean et al., 2004). Given the
869 direct evidence of carnivores recovered on site and the presence of carnivore pits on recovered

specimens (**Fig. 15K**) however, it is plausible to suggest that the relative low abundance of these appendicular elements may have resulted from removal and/or destruction by scavengers; the presence of "sharp" breaks to specimens (**Fig. 15F, H and J**) suggests that trampling by large animals may also have been a destructive factor.

Fig. 15. Examples of fossil crania and post-crania of *Oryx* sp. from Ti's al Gadah. TAG13/109 right maxilla and tooth row in A: lateral and B: occlusal views. TAG13/147, right mandible and tooth row in C: lateral and D: occlusal views. E: TAG14/216, right horn core and cranial fragment, anterior aspect. F: TAG13/099, left humerus cranial view. G: TAG14/901, complete left metatarsal, dorsal view. H: TAG14/195, fragment of distal left tibia, ventral view. I: TAG14/1518 left astragalus, dorsal aspect. J: TAG13/003 distal metacarpal fragment, dorsal view. K: TAG14/205, rib fragment with carnivore pits. Scale bars = 50 mm.

Cheek teeth are robust and hypsodont (**Fig. 15A-D**) although on all fully-erupted adult teeth in wear abrasion appears to have been considerable (**Fig. 15B**), which we interpret to reflect the presence

884 of abrasives (i.e. sand) in the diet. In all examined maxillary tooth rows, the occlusal morphology is
885 simple and we concur with the observations of Thomas et al. (1998) that the dental morphology of the
886 specimens from Ti's al Ghadah is more similar to extant desert-dwelling species, *O. leucoryx* and *O.*
887 *dammah*, rather than *O. gazella* or *O. beisa*. Accessory columns on the lingual face of upper molars are
888 present in *O. gazella* and *O. beisa* but are poorly developed (if present at all) in *O. dammah* and *O.*
889 *leucoryx* and these characters are not present or prominent in the specimens from Ti's al Ghadah (**Fig.**
890 **15B**).

891 Further examination of maxilla fragments indicates that the infra orbital foramen is located
892 posteriorly to P^2, as in the genus, although the posterior palatine foramen appears to be located more
893 distally in the fossil specimens, than in comparative material. The curved edge of the posterior palatine
894 encroaches mesially in line with the M^3 in *O. beisa*, *O. dammah*, and *O. gazella*, but it does not extend
895 beyond the posterior column of the M^3 in comparative material for *O. leucoryx* or the specimens from
896 Ti's al Ghadah (**Fig. 15B**).

897 A small sample of horn-cores (e.g. **Fig 15E**) are characteristic of the genus and rounded in
898 cross-section, although are rather robust in comparison with available reference material (basal
899 measurements: anterior-posterior mean = 43.00 mm; medial lateral mean 41.15 mm, $n = 4$). Thomas et
900 al. (1998) report that Nefud specimens differ from extant *Oryx* spp. by degree of horn core divergence
901 of ca. 35° (Thomas et al. 1998, 149). From the small number of newly recovered specimens ($n = 4$) we
902 estimate a divergence of closer to 20°, but the degree of divergence appears greater than available
903 comparative material for *O. dammah* and *O. leucoryx* and closer to *O. gazella*.

904 Elements from the post cranial skeleton appear to be relatively large and robust (**Table S6**
905 **supplementary data**). A morphometric examination of the maximum dimensions of proximal
906 ephiphyses of fossil metapodia was employed as an index to consider relative body size with available
907 data from extant taxa. While sample sizes of comparative data from *O. leucoryx* are small,
908 measurements of metacarpals (**Fig. 16A**) and metatarsals (**Fig. 16B**) indicate that the specimens from
909 Ti's al Ghadah were larger animals than the endemic species and approach the size of equivalent
910 measurements of *O. beisa*.

911

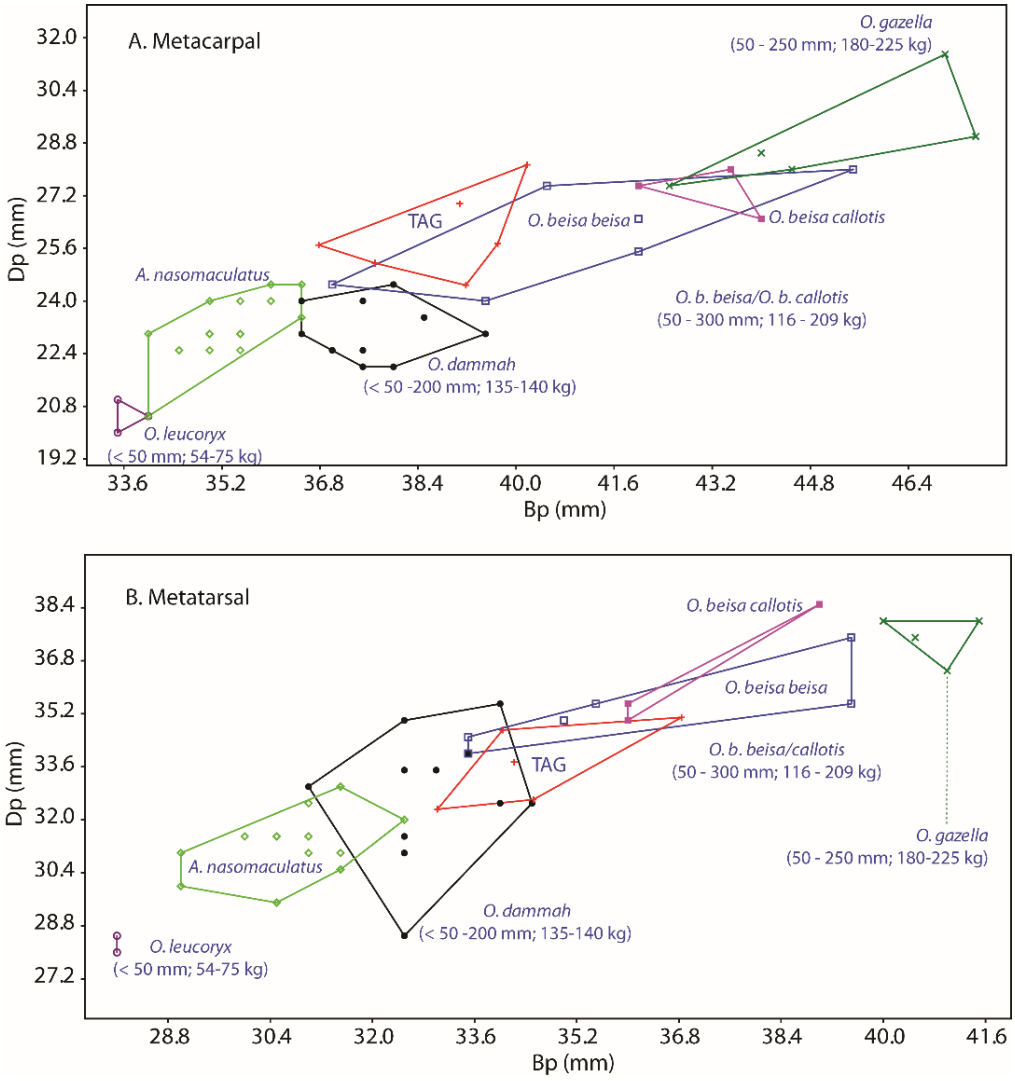

912

913 **Fig. 16.** Measurements of proximal metapodia from fossil *Oryx* sp. from Ti's al Ghadah with comparative
914 morphometric data from four extant *Oryx* spp. and *Addax nasomaculatus*. A: proximal breadth (Bp) and proximal
915 depth (Dp) of metacarpals. B: proximal breadth (Bp) and proximal depth (Dp) of metatarsals. Morphometric data
916 compiled from Peters et al. (1997). Ranges of annual rainfall within *Oryx* spp. extant distributions and body weight
917 ranges (from Stanley Price, 1989, 29) are also annotated. Convex hulls fitted in PAST (Hammer et al., 2001).

918 In summary, the fossil specimens recall O. leucoryx in tooth and palatine morphology, but
919 appear to differ in horn-core characteristics. The available data suggest that the Middle Pleistocene oryx
920 at Ti's al Ghadah were larger and more robust animals than the extant Arabian endemic and closer in
921 size to extant O. beisa. We withhold a species attribution, but suspect that the oryx of Ti's al Ghadah
922 represents a larger-bodied Pleistocene form of the extant endemic.

923

4.3 Chronology

4.3.1 Optically Stimulated Luminescence

TAG1-OSL4 aliquots are 'well-behaved' according to standard SAR protocol rejection criteria, and signal saturation in one aliquot suggests that the pIRIR290 protocol is yielding a stable luminescence emission without the need for fading correction. Given that all other aliquots were unsaturated, though, age underestimation due to signal saturation is not a concern for this sample. Equivalent dose overdispersion (23.8 ± 7.1 %) is among the lowest values measured with the same protocol for similar samples in the Nefud (Clark-Balzan et al., in prep; White et al., in prep). This level of overdispersion both supports the assumption of signal stability, as fading values vary significantly between feldspar grains from the Rub' al Khali (Trauerstein et al., 2012) and would be unlikely to average each other so precisely, and suggests that partial bleaching is a negligible issue. The palaeolake sediments capping the ridge (Unit 7) have a luminescence age of 291 ± 34 ka (**Table 8**).

Table 8

Luminescence dating results for sample TAG1-OSL4. A: pIRIR290 equivalent dose measurements: number of aliquots excluded according to each rejection criterion, and central age model values calculated for the accepted population. B: Values for dose rate calculations and the final sample age.

	Sample	Meas. (#)	Number Rejected			Accepted (#)	CAM D_e (Gy)	Overdispersion (%)
			RR	Zero	Sat.			
A	TAG1-OSL4	10	0	1	1	8	628.6 ± 57.8	23.8 ± 7.1

	Sample	Sample Composition			Burial Depth (m)	Internal Dose Rate (Gy ka^{-1})	Total Wet Dose Rate (Gy ka^{-1})	Age (ka)
		K (%)	Th (ppm)	U (ppm)				
B	TAG1-OSL4	0.41	3.4	1.8	0.25	0.91 ± 0.15	2.16 ± 0.16	291 ± 34

'RR': The ratio of the repeated dose step to the first given dose ('recycling ratio')
'Zero': The ratio of the normalized OSL response of the zero dose step to the natural signal ('zero ratio')
'IR': The ratio of the post-IR repeated dose step to the first given dose ('IR depletion ratio')
'Sat': Aliquots were considered to be saturated if the natural response plus error was greater than the fitted exponential (i.e. Analyst returns an infinite error).

4.3.2 U-series dating

U-series results are shown in **Tables 9** and **10** for samples 3536 and 3538 and in supplementary information (**Tables S7 – S9**) for the other teeth. The tooth samples have unusually high uranium concentrations, on average between 2.0 ppm (3536) and 61.1 ppm (3540) in the enamel and from 139 ppm (3536) to 188 (3540) in the dentine.

947 **Table 9**

948 U-series results on sample 3536. Negative U/Th are due to the background being higher than the measurement.

949 n/a: age calculations not possible, leaching is indicated. All errors are 2-σ.

Sample 3536									
Spot	U (ppm)	Th (ppb)	U/Th	$^{230}Th/^{238}U$	$^{230}Th/^{238}U$ error	$^{234}U/^{238}U$	$^{234}U/^{238}U$ error	Age (ka)	Age error (ka)
1	1.41	-0.2	-6337	0.8490	0.0293	1.1960	0.0176	128.4	9.0
2	1.55	0.3	5380	1.1222	0.0322	1.0588	0.0154	n/a	
3	1.64	-0.7	-2443	1.0063	0.0390	1.0548	0.0151	304.6	68.0
4	2.60	0.3	9061	0.9908	0.0270	1.0888	0.0126	241.2	25.9
5	2.83	0.4	7240	1.0468	0.0290	1.0955	0.0175	291.2	46.5
6	132.0	1.2	110175	1.8516	0.0114	1.6562	0.0030	405.1	17.6
7	133.4	1.6	84429	2.0311	0.0090	1.6984	0.0040	n/a	
8	145.3	1.3	107694	2.1153	0.0084	1.7224	0.0059	n/a	
9	131.23	1.2	112505	2.0140	0.0233	1.6885	0.0071	n/a	
10	152.0	2.3	67061	1.9047	0.0155	1.6095	0.0035	n/a	
11	204.7	18.4	11125	1.6274	0.0100	1.4786	0.0054	430.4	26.6
Mean values									
1-5 Enamel	*2.01 ±0.29*			*1.0096*	*0.0242*	*1.0955*	*0.0112*	*251.0*	*25*
6-10 Dentine	*138.8 ±4.2*			*1.9837*	*0.0075*	*1.6741*	*0.0027*	*n/a*	

950

951 **Table 10**

952 U-series results on sample 3538. Negative U/Th are due to the background being higher than the measurement.

953 n/a: age calculations not possible, leaching is indicated. All errors are 2-σ.

Sample 3538									
Spot	U (ppm)	Th (ppb)	U/Th	$^{230}Th/^{238}U$	$^{230}Th/^{238}U$ error	$^{234}U/^{238}U$	$^{234}U/^{238}U$ error	Age (ka)	Age error (ka)
1	0.9	0.0	166300	0.5428	0.0290	1.2435	0.0270	61.3	4.7
2	4.8	0.1	37935	1.0823	0.0141	1.3052	0.0104	170.7	6.0
3	3.2	0.2	18040	1.0047	0.0221	1.1484	0.0137	206.0	15.0
4	2.8	-0.1	-45258	1.1074	0.0328	1.1622	0.0107	269.6	33.6
5	4.4	1.2	3705	1.3042	0.0263	1.3248	0.0131	272.9	23.9
6	11.6	0.3	36259	1.1768	0.0185	1.1827	0.0079	321.0	29.9
7	137.0	3.4	40150	1.8820	0.0141	1.5268	0.0059	n/a	
8	140.5	3.1	45896	1.9089	0.0117	1.5597	0.0022	n/a	
9	145.5	5.6	26034	1.9141	0.0133	1.5738	0.0048	n/a	
10	164.5	6.9	23999	1.7657	0.0116	1.5362	0.0029	714.2	185.2
11	213.0	11.5	18540	1.4530	0.0078	1.4416	0.0049	279.8	7.0
Mean values									
1-6 Enamel	*4.62 ±1.50*			*1.1321*	*0.0115*	*1.2223*	*0.0064*	*234.7*	*8.9*
7-11 Dentine	*160.1 ±14.1*			*1.7545*	*0.0070*	*1.5204*	*0.0020*	*n/a*	

954

Two tissues show evidence of apparent uranium leaching (3536 dentine and 3538 dentine), for which U-series age cannot be calculated. The enamel sections show consistent mean apparent U-series ages ranging from 235.2 ± 5.8 ka to 268.2 ± 12.3 ka, whereas dentine results are somewhat more scattered from 205.3 ± 4.0 ka to 348.1 ± 11.1 ka. U-series results on skeletal materials have generally to be regarded as minimum age estimates (Grün et al., 2014). The finite dentine ages indicate that the minimum age of the faunal remains within Unit 5 is around 350 ka.

4.3.3 Combined US-ESR dating

Only two fossil teeth were dated by means of the combined US-ESR approach (samples 3536 and 3538) as all the other samples show U-concentration values in enamel > 5 ppm, which is known to be a major issue for accurate age estimation (see Duval et al., 2012). The results of the age calculations are shown in **Table 11**. The samples display characteristics that are usually found in Early Pleistocene teeth: extremely high D_E values (>3500 Gy), apparent U-leaching in dentine, and high U-concentration values in dentine and enamel. Age calculations were performed by assuming early U uptake for the dentine that showed U-leaching (i.e. p= -1). Combined US-ESR age calculations yielded 473+50-33 ka and 554+79-76 ka for samples 3536 and 3538, respectively, resulting in a mean value of 512±59 ka (1-σ error).

Table 11

ESR parameters and combined ESR-U-series age calculations for samples 3536 and 3538.

	Int. dose rate (µGy/a)	Beta dose rate dentine (µGy/a)	Beta dose rate sediment (µGy/a)	Gamma dose rate + cosmic (µGy/a)	Total dose rate (µGy/a)	Enamel thick. (µm)	Removed surface layer (µm) on each side	D_E (Gy)	p-parameter		US-ESR age (ka)
									En.	De.	
3536	213 ±405	8905 ±1317	32 ±15	336 ±35	9485 ±1378	800 ±80	20 ±2	4457 ±399	-0.83	-1	470 +50/-32
3538	1425 ±707	5125 ±863	24 ±12	336 ±35	6910 ±1116	1100 ±110	20 ±2	3831 ±535	-0.58	-1	554 +79/-76

5. Discussion

The vertebrate record of Ti's al Ghadah is an important step toward our understanding of the Pleistocene biogeography in the Arabian Peninsula. While we are mindful that these records derived from a single

site, we consider the wider chronological context of the identified taxa with regional biostratigraphic records and then describe the palaeoecological and palaeoenvironmental inferences that may be drawn from the inferred ecological characteristics of the fauna.

5.1 Chronological context

Our initial interpretation of the formation of the Unit 5 assemblages was that they derived from animals moving into the basin with the onset of wetter conditions and that the overlying lake deposit in the ridge, as observed in section (Unit 7; see Fig. 4), represented a later expansion of a contemporaneous lake formation (Stimpson et al., 2015). The earlier work by Rosenberg et al. (2013) suggested a date equivalent to MIS 9.

The OSL date from the "capping" lacustrine deposits of the ridge, however, suggests that this formation was later, likely MIS 7. Conversely, U-series analyses of oryx teeth from Unit 5 suggest a minimum age for the Unit 5 fossils of ca. 350 ka and combined US-ESR dating indicates on older age and that the assemblages derived from ca. 500 ka, likely MIS 11. A strict interpretation of the available dating information would be that the Unit 5 assemblages derived from animals associated with an earlier phase of lake formation, not represented in section in the ridge, and that there was significant erosion and/or depositional hiatuses after the formation of the Unit 5 stratum and the overlying lacustrine deposits in the ridge. We suspect that the iron-rich, relict lake deposit in the centre of the basin (section 4.1) represents the contemporaneous lake and the key water resource for faunal populations from which the Unit 5 assemblages derived.

5.2 Biogeographical and biostratigraphical implications of the Ti's al Ghadah fauna

The fossils of Ti's al Ghadah include the first Pleistocene-age bird bones to be reported from the Arabian Peninsula. In terms of biostratigraphy their utility is limited, except to say the identified species are relatively early records and are known from regional records today (Porter and Aspinall, 2010).

The extinct *Panthera gombaszogensis* is regarded as Eurasian taxon and is known from the Early to Middle Pleistocene (e.g. Marciszak, 2014). Records for this enigmatic fossil felid are sparse in SW Asia. The specimens from Ti's al Ghadah are the most southerly known records of this taxon,

1007 although with the present dating information for the site these records fit well within the chronological
1008 range of this taxon. The Eurasian jaguar is known from the Kudaro faunal unit (MIS 9-11) in the
1009 Caucasus and is described from Layer 5c from Kudaro 1, which yielded two thermoluminescence dates
1010 of 360 ± 90 ka and 350 ± 70 ka (Baryshnikov, 2002).

1011 We infer the presence of the spotted hyeana (currently restricted to Sub-Saharan Africa) at Ti's
1012 al Ghadah from coprolites. A well-preserved mandible is an unequivocal fossil record from elsewhere
1013 in the southwestern Nefud Desert, from Locality # 3 (Thomas et al., 1998). It is likely that this locality
1014 is site 16.1 of Rosenberg et al. (2013), which yielded OSL dates between 419 ± 39 ka and 286 ± 30 ka
1015 (Table 1). While there is no strict evidence of any chronological affinity between Locality # 3 and Ti's
1016 al Ghadah, the inferred presence of these predators at Ti's al Ghadah is further indication of a Middle
1017 Pleistocene context for this species. The spotted hyena is known from Levantine sites until at least the
1018 Middle Pleistocene (e.g. Bar-Yosef and Belmaker, 2011) and it appears that it was also a component of
1019 the fauna of the Arabian Peninsula during this time.

1020 The biogeographic implications of the record of the African golden wolf, *Canis anthus*, are
1021 more difficult to consider as the taxonomic affinity of this cryptic canid was clarified only recently.
1022 This species clearly has a larger extant geographic range in Africa than previously thought and the
1023 record from Ti's al Ghadah suggests that it ranged into the Arabian Peninsula in the Middle Pleistocene.

1024 The extinct elephant, *Palaeoloxodon recki*, is known from the Middle Pliocene until the Middle
1025 Pleistocene in Africa, where it is conventionally divided into five chronological stages. The elephants
1026 of Ti's al Ghadah are morphologically consistent with the latest stage of *P. recki*, *P. recki recki*, with
1027 known occurrence in East Africa between ca. 1.5-0.4 Ma, although it is not possible to rule out an earlier
1028 stage for the small sample of two molars: the potentially diagnostic specimen (the M^3) is incomplete.
1029 After 0.5 Ma, the African species *P. iolensis*, is believed to be the lineal descendent of *P. recki* and
1030 persists until the Late Pleistocene, possibly as late as 75 ka (Sanders et al., 2010). *P. iolensis* lack the
1031 median enamel expansions of *P. recki* that are also seen in the molars from Ti's al Ghadah. However,
1032 that a population of the *recki-iolensis* lineage existed in the Arabian peninsula in the Middle Pleistocene
1033 is perfectly plausible.

A descendant of *Palaeoloxodon recki*, *P. antiquus,* is known from Europe from Middle to Late Pleistocene (ca. 780 to 50 ka), where it underwent relatively little evolutionary change before going extinct during the last glaciation (Lister, 2004, 2016). *Palaeoloxodon antiquus* has also been identified in the Levant. A *Palaeoloxodon* cranium from Gesher Benot Ya'aqov (GBY), Israel, dated to 780 ka, has been regarded as one of the earliest representatives of this species, and the species has also been identified at Revadim Quarry ("ca. 500-300 ka or possibly more": Rabinovich et al., 2012). However, Saegusa and Gilbert (2008), on the basis of cranial characters, suggested that the GBY cranium might actually be *P. recki*, while the morphology of the Revadim elephants has not been described in sufficient detail to discriminate between the two species. The taxonomic boundary between *P. recki* and *P. antiquus*, in this geographical region and time-interval, is therefore currently blurred, but it cannot be ruled out that the elephants of Ti's al Ghadah might have derived from Europe and eventually be considered to belong to *P. antiquus.*

Further samples from Ti's al Ghadah are required to clarify the range of the equid taxa that are represented at the site, although our identification of a mandible of *E. hemionus* is consistent with regional fossils records. *Equus hemionus* appears as part of fauna of SW Asia and the Levant in the Middle Pleistocene. Specimens are reported from Nadaouiyeh Aïn Askar (El Kown) in Syria (Savioz and Morel, 2005) and from Levantine sites (Bar-Yosef and Belmaker, 2011) and dated to 300-500 ka, and 100-300 ka, respectively.

We suspect that the *Oryx* sp. of Ti's al Ghadah is likely to be a large but closely-related Pleistocene form of the extant endemic *Oryx leucoryx*. Ancestral populations were probably established in the Miocene and these antelopes will likely have been a long-standing presence in the Arabian Peninsula. Fossils of this genus have proved to be common in Pleistocene assemblages of different ages in the southwestern Nefud Desert (Thomas et al., 1998; White et al., forthcoming).

5.3 Vertebrate palaeoecology and palaeoenvironments and at Ti's al Ghadah.

The identified taxa indicate that the Ti's al Ghadah basin was, at least at times, a focal point in the landscape for birds, herbivorous mammals and predators and scavengers. However, given that there have been suggestions that Pleistocene lacustrine deposits in the Nefud Desert may represent ephemeral

marsh-like habitats, rather than the formation of substantial bodies of water (Enzel et al., 2015), this raises the question of whether the Unit 5 assemblages represent animals that were attracted to an ephemeral water source and a relatively brief flush of plants in the dune fields, or were these resources more substantial and long-standing at Ti's al Ghadah or in the wider Nefud Desert?

At present, it is not possible to determine the degree of time-averaging of the Unit 5 assemblages, although the fossil stratum appears to be a rather discrete unit with little evidence of significant reworking or redeposition. There is clear evidence, however, of a least three discrete episodes of the formation of standing water within the Ti' al Ghadah basin and there is regional evidence of the periodic formation of water bodies throughout southwestern Nefud Desert dating from the Middle Pleistocene onward (Rosenberg et al., 2013; White et al., forthcoming). Rosenberg et al. (2013) suggest the possibility that large-scale lake and wetland habitats developed across the western Nefud during MIS 11. The inferred presence of a lake at Ti's al Ghadah would be supported by previous reports of a fossil of a relatively large Osteoglossiforme fish (although his was an unstratified specimen) and consistent with the aquatic affinities of two of the identified avian taxa (grebe, duck). Indeed, the presence of the bird taxa identified at the site may parsimoniously be explained as attracted to habitat (grebe, duck, wagtail), to drink (sandgrouse, ostrich) or in a scavenging role (Egyptian vulture, kite).

Oryx, equids and elephant will likewise have been attracted to fresh water and plant resources and we infer that the remains recovered in Unit 5 reflect die-off in populations of these animals. Animal carcasses will have attracted mammalian scavengers such as fox, wolf and hyaena and the attention of carnivores is evidenced by tooth marks. Although it was not possible to identify to the reptilian fossils to genus it is worth noting that, in this context, the majority of extant *Varanus* spp. are carnivorous and will scavenge animal carcasses, whereas *Uromastyx* spp. are primarily herbivorous. It is plausible that the Egyptian vulture also scavenged at the site, but it is notable that one of these birds were in turn subject to the attentions of a carnivore.

The establishment of water holes has been shown to have a significant effect on the hunting behaviour of large felids (e.g. Valeix et al., 2010) and the presence of a large-bodied pantherine (ca. 100 kg: see Stimpson et al., 2015) suggests that the biomass of potential vertebrate prey would likely have been substantial in the area (e.g. Carbone and Gittleman, 2002) as would, by inference, plant

resources. We also infer the presence of hyeana (cf. *Crocuta crocuta*) from coprolites. While these animals are famed as scavengers and for the demolition of bone, they are dynamic and capable predators. Modern analogues should be applied with caution but it is notable that the taxonomic and ecological composition of the fossil fauna from Ti's al Ghadah bears some resemblance to Namibian desert ecosystems that experience flushes of plant growth in response to increased precipitation. For example, increased wetting prompts a seasonal influx of large number of gemsbok (*Oryx gazella*) to the Kuiseb river from surrounding dunefields (Kok and Nel, 1996) and these antelopes and the mountain zebra (*Equus zebra hartmannae*) are important prey animals for local populations of spotted hyaena (Tilson and Henschel, 1986).

For the *Palaeoloxodon* remains, there is clearly more than one individual preserved at the site: further excavation is likely to reveal the remains of further elephants and may allow assessment of the age profile of the assemblage, with possible relevance to mode of accumulation. *Palaeoloxodon recki* and *P. antiquus* are estimated to have had a body mass of ca. 10-12 tonnes (Larramendi, 2015) and would have been a social animal living in family groups like living elephants. Elephants require a substantial intake of water (up to 360 litres a day in an adult), implying local availability of water. Elephants in semi-desert areas of Africa (Mali and Namibia) undertake substantial migrations in search of food and water, and focus on moist riverside vegetation (e.g. Viljoen, 1989a, b) but Ramey et al. (2013) have demonstrated a reliance on clean, un-fouled water resources.

While the fossil elephants of the Nefud were not necessarily there year round, but perhaps only when food and water supplies allowed, a substantial biomass of vegetation is required to support an elephant herd, even though elephants can survive on relatively low-quality herbage. Microwear and isotopic studies of *Palaeoloxodon* indicate a mixed-feeder taking both graze and browse (Grube et al., 2010; Rivals et al. 2012). The mesowear method of Saarinen et al. (2015) has been applied to the upper molar (TAG14/301) and lower dP_4 (TAG14/281) from Ti's al Ghadah: the former gave an average mesowear angle of 120°, indicating a grass-dominated mixed-feeder (50-70 % grass); the latter an angle of 136°, indicating a strongly graze-dominated diet (> 90 % grass).

The presence of a robust hemione and the feeding habits of extant oryx species are also suggestive of the presence of open, grassland habitats. Extant oryx species are mixed feeders although

the majority of the diet consists of coarse grasses occasionally supplemented by ephemeral forbs (Stanley-Price, 1989). The Pleistocene oryx of Ti's al Ghadah, however, appears to have been a relatively large-bodied form and available data indicates that the specimens approach the size of the extant *O. beisa*. While *Oryx* spp. display marked physiological adaptations to tolerate drought conditions (e.g. Ostrowski et al., 2006), available data for four species indicate that there is a broad but positive correlation between annual rainfall and body weight (**Fig. 16**). It is plausible to suggest that the relative size of the oryx of Ti's al Ghadah reflected more amenable habitats and that climatic and environmental amelioration was of a sufficient duration to support populations of this larger-bodied form.

6. Conclusion

The Middle Pleistocene fauna of Ti's al Ghadah reported here, dated to ca. 500 ka, comprises of reptiles, birds and mammals. The bird fossils are the first Pleistocene-age records to be reported from the Arabian Peninsula. The mammalian fauna consists of an admixture of African, Eurasian and likely endemic taxa, which we interpret to reflect the geographic situation of the Arabian Peninsula as a crossroads between continents. The identified vertebrate taxa indicate that areas of the southwest Nefud Desert in MIS 11 held (at least periodically) substantial freshwater and plant resources and were a focal point in the landscape for birds and populations of herbivores (including very large mammals) and their predators and scavengers.

Acknowledgements

For permission to conduct this study, we thank HRH Prince Sultan bin Salman, President of the Saudi Commission for Tourism and National Heritage (SCTH) and Professor Ali I. Al-Ghabban, Vice President. We thank Jamal Omar and Sultan Al-Fagir of the SCTH for their support and assistance with the field investigations. Particular thanks to Abdullah Alsharekh of King Saud University for discussions and long term support. We thank Heidi Eager, Muhammed Zahir, Oshan Wedage, Marco Bernal, Patrick Cuthbertson, Patrick Roberts, Margaret Ashley-Veall and Helena White (Palaeodeserts) and Saleh A. Soubhi, Mohammed A. Haptari, Adel H. Matari, Abdu M. Al-Masary, Ahmad A.

Bahameem and Ammar Jamal Jamalaldeen (Saudi Geological Survey) for their contributions in the field. Sandra Chapman and Pip Brewer provided access to comparative specimens at the Natural History Museum (Palaeontology), as did Jo Cooper and Judith White at the Bird Group in Tring. CMS thanks Jo Cooper for helpful discussion. Malgosia Nowak-Kemp and Eliza Howlett assisted with access to specimens in the Oxford University Museum of Natural History (OUMNH) and CMS is grateful to Darren Mann and Bethany Columbo for permission and assistance while working in the osteological collections. Jess Rippengal helped with access to the reference collections in Cambridge, as did Malcolm Pearch at the Harrison Institute (Sevenoaks). We thank Nigel Larkin for his conservation work on TAG14/301 and his advice on the identification of hyaena coprolites; discussions with Simon Parfitt were also particularly helpful in this regard. Juha Saarinen kindly measured the mesowear angles of the elephant molars, and provided discussion. This study also benefited from discussions with Chris Jarvis (OUMNH), Matt Freidman and Roger Benson (University of Oxford). We thank Heidi Eager and Laura Bishop for valuable and constructive comments on an early draft of the manuscript. CMS thanks Ian Cartwright for the photographs of specimens shown in Figs. 10A and B and 15A and B. The ESR dating study has received funding from a Marie Curie International Outgoing Fellowship of the European Union's Seventh Framework Programme (FP7/2007-2013) awarded to MD under REA Grant Agreement nº PIOF-GA-2013-626474. MDP acknowledges financial support from the European Research Council (grant no. 295719, to MDP) and from the SCTH. Author contributions: CMS wrote the paper, with contributions from all authors; fossil analysis was undertaken by CMS (except elephant fossils) and AL (elephant fossils); Stratigraphic analysis was undertaken by AP; OSL dating was undertaken by LCB; U-series and ESR dating was undertaken by MD and RG; Mapping, and site survey was undertaken by PB; RJ collated fossil survey data; study was conceived by MDP and supervised in the field by AA-O and RJ (2013) and AA-O, KSMAM, CMS, ISZ, YAM and AMM (2014).

References

Adamiec, G., Aitken, M. J., 1998. Dose-rate conversion factors: update. Ancient TL 16 (2), 37-50.

Alberdi, M. T., Palombo, M. R., 2013. The late Early to early Middle Pleistocene stenonoid horses from Italy. Quaternary International 288, 25-44. http://dx.doi.org/10.1016/j.quaint.2011.12.005.

1176 Andrews, P., Whybrow, P., 2005. Taphonomic observations on a camel skeleton in a desert environment in Abu
1177 Dhabi. Palaeontologia Electronica 8 (1), 23A, 17p.
1178
1179 Armitage, S. J., Jasim, S. A., Marks, A. E., Parker, A. G., Usik, V. I., Uerpmann, H. P., 2011. The southern
1180 route "Out of Africa": evidence for an early expansion of modern humans into Arabia. Science 331 (6016), 453-
1181 456. http://dx.doi.org/10.1126/science.1199113.
1182
1183 Azzaroli, A., Stanyon, R., 1991. Specific identity and taxonomic position of the extinct Quagga. Rendiconti
1184 Lincei 2 (4), 425-436. http://dx.doi.org/10.1007/bf03001000.
1185
1186 Bar-Yosef, O., Belmaker, M., 2011. Early and Middle Pleistocene faunal and hominins dispersals through
1187 Southwestern Asia. Quaternary Science Reviews 30 (11), 1318-1337.
1188 http://dx.doi.org/10.1016/j.quascirev.2010.02.016.
1189
1190 Baryshnikov, G. F., 2002. Local biochronology of Middle and Late Pleistocene mammals from the Caucasus.
1191 Russian Journal of Theriology 1 (1), 61-67.
1192
1193 Baryshnikov, G.F., 2012. Pleistocene Canidae (Mammalia, Carnivora) from the Paleolithic Kudaro caves in the
1194 Caucasus. Russian Journal of Theriology 11 (2), 77-120.
1195
1196 Baryshnikov, G.F., Tsoukala, E., 2010. New analysis of the Pleistocene carnivores from Petralona Cave
1197 (Macedonia, Greece) based on the collection of the Thessaloniki Aristotle University. Geobios 43, 389-402.
1198 http://dx.doi.org/10.1016/j.geobios.2010.01.003.
1199
1200 Baumel J. J., Witmer L. M., 1993. Osteologia. In: Baumel J. J., King A. S., Breazile J. E., Evans H. E., Vanden
1201 Berge J. C. (Eds.), Handbook of Avian Anatomy: Nomina Anatomica Avium. Publications of the Nuttall
1202 Ornithological Club 23, Cambridge, Massachusetts, pp. 45–132.
1203
1204 Beden, M., 1979. Les éléphants (*Elephas* et *Loxodonta*) d'Afrique orientale: systématique, phylogénie, intéret
1205 biochronologique. Thèse de Doctorat d'Etat. Poitiers.
1206
1207 Beech, M. J., Hellyer, P., 2005. Abu Dhabi-8 Million Years Ago: Late Miocene Fossils from the Western
1208 Region. Abu Dhabi Islands Archaeological Survey (ADIAS).
1209
1210 Behrensmeyer, A.K., 1978. Taphonomic and ecologic information from bone weathering. Paleobiology 4 (2),
1211 150-162.
1212
1213 Belmaker, M., 2009. Hominin adaptability and patterns of faunal turnover in the Early to Middle Pleistocene
1214 transition in the Levant. In: Camps, M., Chauhan, P.R. (Eds.), Sourcebook of Paleolithic Transitions. Springer,
1215 New York, pp. 211-227. http://dx.doi.org/10.1007/978-0-387-76487-0_12.
1216
1217 Beyin, A., 2006. The Bab al Mandab vs the Nile-Levant: an appraisal of the two dispersal routes for early
1218 modern humans out of Africa. African Archaeological Review 23 (1-2), 5-30. http://dx.doi.org/10.1007/s10437-
1219 006-9005-2.
1220
1221 Breeze, P.S., Drake, N.A., Groucutt, H.S., Parton, A., Jennings, R.P., White, T.S., Clark-Balzan, L., Shipton, C.,
1222 Scerri, E.M.L., Stimpson, C.M., Crassard, R., Hilbert, Y., Alsharekh, A., Al-Omari, A., Petraglia, M.D., 2015.
1223 Remote sensing and GIS techniques for reconstructing Arabian palaeohydrology and identifying archaeological
1224 sites. Quaternary International 382, 98-119. http://dx.doi.org/10.1016/j.quaint.2015.01.022.
1225
1226 Brennan, B. J., 2003. Beta doses to spherical grains. Radiation Measurements 37 (4), 299-303.
1227 http://dx.doi.org/10.1016/s1350-4487(03)00011-8.
1228
1229 Brennan, B.J., Lyons, R.G., Phillips, S.W., 1991. Attenuation of alpha particle track dose for spherical grains.
1230 International Journal of Radiation Applications and Instrumentation. Part D. Nuclear Tracks and Radiation
1231 Measurements 18, 249-253. http://dx.doi.org/10.1016/1359-0189(91)90119-3.
1232
1233 Brugal, J-P., Boudadi-Maligne, M., 2011. Quaternary small to large canids in Europe: taxonomic status and
1234 biochronological contribution. Quaternary International 243, 171-182.
1235 http://dx.doi.org/10.1016/j.quaint.2011.01.046.

Burchak-Abramovich, N. I., Vekua, A. K., 1990. The fossil ostrich *Struthio dmanisensis* sp. n., from the Lower Pleistocene of Georgia. Acta zoologica cracoviensia 33 (7), 121-132.

Carbone, C., Gittleman, J.L., 2002. A common rule for the scaling of carnivore density. Science 295, 2273-2276. http://dx.doi.org/10.1126/science.1067994.

Cox, N. A., Mallon, D., Bowles, P., Els, J., Tognelli, M. F., (compilers) 2012. The Conservation Status and Distribution of Reptiles of the Arabian Peninsula. Cambridge, UK and Gland, Switzerland: IUCN, and Sharjah, UAE: the Environment and Protected Areas Authority.

Delagnes, A., Tribolo, C., Bertran, P., Brenet, M., Crassard, R., Jaubert, J., Khalidi, L., Mercier, N., Nomade, S., Peigné, S., Sitzia, L., Tournepiche, J.-F., Al-Halibi, M., Al-Mosabi, A., Macchiarelli, R. 2012. Inland human settlement in southern Arabia 55,000 years ago. New evidence from the Wadi Surdud Middle Paleolithic site complex, western Yemen. Journal of Human Evolution 63 (3), 452-474. http://dx.doi.org/10.1016/j.jhevol.2012.03.008.

Delagnes, A., Crassard, R., Bertran, P., Sitzia, L., 2013. Cultural and human dynamics in southern Arabia at the end of the Middle Paleolithic. Quaternary International, 300, 234-243. http://dx.doi.org/10.1016/j.quaint.2012.12.012.

Delany, M. J., 1989. The zoogeography of the mammal fauna of southern Arabia. Mammal Review 19 (4), 133-152. http://dx.doi.org/10.1111/j.1365-2907.1989.tb00408.x.

Davis, S. J., 1980. Late Pleistocene and Holocene equid remains from Israel. Zoological Journal of the Linnean Society 70 (3), 289-312. http://dx.doi.org/10.1111/j.1096-3642.1980.tb00854.x.

Dayan, T., 1994. Early domesticated dogs of the Near East. Journal of Archaeological Science, 21 (5), 633-640. http://dx.doi.org/10.1006/jasc.1994.1062.

Dayan, T., Simberloff, D., Tchernov, E., Yom-Tov, Y., 1992. Canine carnassials: character displacement in the wolves, jackals and foxes of Israel. Biological Journal of the Linnean Society, 45 (4), 315-331. http://dx.doi.org/10.1111/j.1095-8312.1992.tb00647.x.

Dennell, R., Petraglia, M.D., 2012. The dispersal of Homo sapiens across southern Asia: how early, how often, how complex? Quaternary Science Reviews 47, 15-22. http://dx.doi.org/10.1016/j.quascirev.2012.05.002.

Dobney, K., Beech, M., Jaques, D., 1999. Hunting the broad spectrum revolution: the characterisation of early Neolithic animal exploitation at Qermez Dere, northern Mesopotamia. In: Driver, J.C. (Ed.), Zooarchaeology of the Pleistocene/Holocene Boundary. BAR International Series 800, Oxford, pp. 47-57.

Duval, M., 2015. Electron Spin Resonance (ESR) dating of fossil tooth enamel. Encyclopedia of Earth Sciences Series, Springer Dordrecht. pp. 239–246. http://dx.doi.org/10.1007/978-94-007-6304-3_71.

Duval, M., Grün, R., 2016. Are published ESR dose assessments on fossil tooth enamel reliable? Quaternary Geochronology 31, 19-27. http://dx.doi.org/10.1016/j.quageo.2015.09.007.

Duval, M., Falguères, C., Bahain, J.-J., Grün, R., Shao, Q., Aubert, M., Hellstrom, J., Dolo, J.-M., Agusti, J., Martínez-Navarro, B., Palmqvist, P., Toro-Moyano, I., 2011. The challenge of dating Early Pleistocene fossil teeth by the combined uranium series–electron spin resonance method: the Venta Micena palaeontological site (Orce, Spain). Journal of Quaternary Science 26, 603-615. http://dx.doi.org/10.1002/jqs.1476.

Duval, M., Falguères, C., Bahain, J.-J., 2012. Age of the oldest hominin settlements in Spain: Contribution of the combined U-series/ESR dating method applied to fossil teeth. Quaternary Geochronology 10(0): 412-417. http://dx.doi.org/10.1016/j.quageo.2012.02.025.

Eggins, S., Grün, R., Pike, A., Shelley, A., Taylor, L., 2003. ^{238}U, ^{232}Th profiling and U-series isotope analysis of fossil teeth by laser ablation ICPMS. Quaternary Science Reviews 22, 1373-1382. http://dx.doi.org/10.1016/s0277-3791(03)00064-7.

1296 Eggins, S.M., Grün, R., McCulloch, M.T., Pike, A.W.G., Chappell, J., Kinsley, L., Mortimer, G., Shelley, M.,
1297 Murray-Wallace, C.V., Spötl, C., Taylor, L., 2005. In situ U-series dating by laser-ablation multi-collector
1298 ICPMS: new prospects for Quaternary geochronology. Quaternary Science Reviews 24, 2523-2538.
1299 http://dx.doi.org/10.1016/j.quascirev.2005.07.006.
1300
1301 Eisenmann, V., Helmer, D., Segui, M. S., 2002. The big *Equus* from the Geometric Kebaran of Umm El Tlel,
1302 Syria: *Equus valeriani*, *Equus capensis* or *Equus caballus*? In: Buitenhuis, H., Choyke, A.M., Maskour, M., Al-
1303 Shiyab, A.H., (Eds.) Archaeolozoology of the Near East V, Proceedings of the Fifth International Symposium
1304 on the Archaeozoology of Southwestern Asia and Adjacent Areas. Groningen, pp. 62-73.
1305
1306 Eisenmann, V., Howe, J., Pichardo, M., 2008. Old World hemiones and New World slender species (Mammalia,
1307 Equidae). Palaeovertebrata 36 (1-4), 159-233.
1308
1309 Fernandes, C. A., 2009. Bayesian coalescent inference from mitochondrial DNA variation of the colonization
1310 time of Arabia by the hamadryas baboon (*Papio hamadryas hamadryas*). In: Petraglia, M.D., Rose, J.I. (Eds.),
1311 The evolution of human populations in Arabia: Paleoenvironments, Prehistory and Genetics. Springer,
1312 Netherlands, pp. 89-100. http://dx.doi.org/10.1007/978-90-481-2719-1_7.
1313
1314 Fernandes, C. A., 2011. Colonization time of Arabia by the White-tailed Mongoose *Ichneumia albicauda* as
1315 inferred from mitochondrial DNA sequences: (Mammalia: Herpestidae). Zoology in the Middle East 54
1316 (supplement 3), 111-124. http://dx.doi.org/10.1080/09397140.2011.10648903.
1317
1318 Fernandes, C. A., Rohling, E. J., Siddall, M., 2006. Absence of post-Miocene Red Sea land bridges:
1319 biogeographic implications. Journal of Biogeography, 33 (6), 961-966. http://dx.doi.org/10.1111/j.1365-
1320 2699.2006.01478.x.
1321
1322 Ferretti, M. P., Ficcarelli, G., Libsekal, Y., Tecle, T. M., Rook, L., 2003. Fossil elephants from Buia (Northern
1323 Afar Depression, Eritrea) with remarks on the systematics of *Elephas recki* (Proboscidea, Elephantidae). Journal
1324 of Vertebrate Paleontology 23, 244–257. http://dx.doi.org/10.1671/0272-4634(2003)23[244:fefbna]2.0.co;2
1325
1326 Fjeldså, J., 2004. The Grebes, Podicipedidae. Oxford University Press, Oxford.
1327
1328 Fleitmann, D., Matter, A., 2009. The speleothem record of climate variability in Southern Arabia. Comptes
1329 Rendus Geoscience, 341 (8), 633-642. http://dx.doi.org/10.1016/j.crte.2009.01.006.
1330
1331 Fleitmann, D., Burns, S. J., Neff, U., Mangini, A., Matter, A., 2003. Changing moisture sources over the last
1332 330,000 years in Northern Oman from fluid-inclusion evidence in speleothems. Quaternary Research, 60 (2),
1333 223-232. http://dx.doi.org/10.1016/s0033-5894(03)00086-3.
1334
1335 Fleitmann, D., Burns, S.J., Pekala, M., Mangini, A., Al-Subbary, A., Al-Aowah, M., Kramers, J., Matter, A.,
1336 2011. Holocene and Pleistocene pluvial periods in Yemen, southern Arabia. Quaternary Science Reviews 30
1337 (7), 783-787. http://dx.doi.org/10.1016/j.quascirev.2011.01.004.
1338
1339 Flower, L. O., Schreve, D. C., 2014. An investigation of palaeodietary variability in European Pleistocene
1340 canids. Quaternary Science Reviews, 96, 188-203. http://dx.doi.org/10.1016/j.quascirev.2014.04.015.
1341
1342 Galbraith, R. F., Roberts, R. G., Laslett, G. M., Yoshida, H., Olley, J. M., 1999. Optical dating of single and
1343 multiple grains of quartz from jinmium rock shelter, northern australia: part I, experimental design and statistical
1344 models. Archaeometry, 41 (2), 339-364. http://dx.doi.org/10.1111/j.1475-4754.1999.tb00987.x.
1345
1346 Gaubert, P., Bloch, C., Benyacoub, S., Abdelhamid, A., Pagani, P., Adéyèmi, C., Sylvestre M., Djagoun, A. C.,
1347 and Dufour, S., 2012. Reviving the African wolf *Canis lupus lupaster* in North and West Africa: a
1348 mitochondrial lineage ranging more than 6,000 km wide. PloS one 7 (8), e42740.
1349 http://dx.doi.org/10.1371/journal.pone.0042740.
1350
1351 Geigl, E. M., Grange, T., 2012. Eurasian wild asses in time and space: Morphological versus genetic diversity.
1352 Annals of Anatomy-Anatomischer Anzeiger, 194 (1), 88-102. http://dx.doi.org/10.1016/j.aanat.2011.06.002.
1353
1354 Geraads, D., 2011. A revision of the fossil Canidae (Mammalia) of north-western Africa. Palaeontology, 54 (2),
1355 429-446. http://dx.doi.org/10.1111/j.1475-4983.2011.01039.x.

1356 Groucutt, H.S., Petraglia, M.D., 2012. The prehistory of the Arabian Peninsula: Deserts, dispersals and
1357 demography. Evolutionary Anthropology 21, 113-125. http://dx.doi.org/10.1002/evan.21308.
1358
1359 Groucutt, H.S., Petraglia, M.D., Bailey, G., Scerri, E.M.L., Parton, A., Clark-Balzan, L., Jennings, R.P., Lewis,
1360 L., Blinkhorn, J., Drake, N.A., Breeze, P.S., Inglis, R.H., Devès, M.H., Meredith-Williams, M., Boivin, N.,
1361 Thomas, M.G., Scally, A., 2015a. Rethinking the dispersal of Homo sapiens out of Africa. Evolutionary
1362 Anthropology 24, 149–164. http://dx.doi.org/10.1002/evan.21455.
1363
1364 Groucutt, H. S., Shipton, C., Alsharekh, A., Jennings, R., Scerri, E. M., Petraglia, M. D. 2015b. Late Pleistocene
1365 lakeshore settlement in northern Arabia: Middle Palaeolithic technology from Jebel Katefeh, Jubbah.
1366 Quaternary International 382, 215-236. http://dx.doi.org/10.1016/j.quaint.2014.12.001.
1367
1368 Groucutt, H.S., White, T.S., Clark-Balzan, L., Parton, A., Crassard, R., Shipton, C., Jennings, R.P., Parker,
1369 A.G., Breeze, P.S., Scerri, E.M.L., Alsharekh, A., Petraglia, M.D. 2015c. Human occupation of the Arabian
1370 Empty Quarter during MIS 5: evidence from Mundafan Al-Buhayrah, Saudi Arabia. 2015b. Quaternary Science
1371 Reviews, 119, 116-135. http://dx.doi.org/10.1016/j.quascirev.2015.04.020.
1372
1373 Grube, R., Palombo, M.R., Iacumin, P., Di Matteo, A., 2010. What did the fossil elephants from Neumark-Nord
1374 eat? In: Meller, H. (Ed.), Elefantenreich – Eine Fossilwelt in Europa. Halle/Saale, pp. 253–273.
1375
1376 Guenther, E. W., 1977. Die Backenzähne der Elefanten von Taubach bei Weimar. Quartärpaläontologie 2, 265-
1377 304.
1378
1379 Grün, R., 2000. Methods of dose determination using ESR spectra of tooth enamel. Radiation Measurements 32,
1380 767-772. http://dx.doi.org/10.1016/s1350-4487(99)00281-4.
1381
1382 Grün, R., 2009. The DATA program for the calculation of ESR age estimates on tooth enamel. Quaternary
1383 Geochronology 4, 231-232. http://dx.doi.org/10.1016/j.quageo.2008.12.005.
1384
1385 Grün, R., Brumby, S., 1994. The assessment of errors in past radiation doses extrapolated from ESR/TL dose-
1386 response data. Radiation Measurements 23, 307-315. http://dx.doi.org/10.1016/1350-4487(94)90057-4.
1387
1388 Grün, R., Katzenberger-Apel, O., 1994. An alpha irradiator for ESR dating. Ancient TL 12, 35-38.
1389
1390 Grün, R., Eggins, S., Kinsley, L., Mosely, H., Sambridge, M., 2014. Laser ablation U-series analysis of fossil
1391 bones and teeth. Palaeogeography, Palaeoclimatology, Palaeoecology 416, 150-167.
1392 http://dx.doi.org/10.1016/j.palaeo.2014.07.023.
1393
1394 Guérin, G., Mercier, N., Adamiec, G., 2011. Dose-rate conversion factors: update. Ancient TL 29, 5-8.
1395
1396 Hammer, Ø.,Harper, D.A.T., 2006. Paleontological Data Analysis. Blackwell Publishing, Oxford.
1397 http://dx.doi.org/10.1002/9780470750711.
1398
1399 Hammer, Ø., Harper, D.A.T., Ryan, P.D., 2001. Paleontological Statistics Software Package for Education and
1400 Data Analysis. Palaeontologia Electronica 4 (1), 9 pp.
1401
1402 Harrison, D. L., Bates, P. J. J., 1991. The mammals of Arabia. Harrison Zoological Museum, Sevenoaks.
1403
1404 Hoffstetter, R. Gasc, J-P. 1969. Vertebrae and ribs of modern reptiles. In: Gans, C. Bellairs, A. d' A., Parsons,
1405 T.S., (Eds.). Biology of the Reptilia Volume 1. Academic Press, New York, pp. 201–310.
1406
1407 Holmes, R. B., Murray, A. M., Attia, Y. S., Simons, E. L., Chatrath, P., 2010. Oldest known Varanus
1408 (Squamata: Varanidae) from the Upper Eocene and Lower Oligocene of Egypt: support for an African origin of
1409 the genus. Palaeontology 53 (5), 1099-1110. http://dx.doi.org/10.1111/j.1475-4983.2010.00994.x.
1410
1411 Huntley, D. J., Baril, M. R., 1997. The K content of the K-feldspars being measured in optical dating or in
1412 thermoluminescence dating. Ancient TL, 15 (1), 11-13.
1413
1414 Huntley, D. J., Hancock, R. G. V., 2001. The Rb contents of the K-feldspar grains being measured in optical
1415 dating. Ancient TL, 19 (2), 43-46.

Huxley, T.H., 1880. On the Cranial and Dental Characters of the Canidæ. Proceedings of the Zoological Society of London 48 (2), 238-288. http://dx.doi.org/10.1111/j.1469-7998.1880.tb06558.x.

Larkin, N.R., Alexander, J., Lewis, M.D., 2000. Using experimental studies of recent faecal material to examine hyaena coprolites from the West Runton Freshwater Bed, Norfolk, UK. Journal of Archeological Science 27, 19-31. http://dx.doi.org/10.1006/jasc.1999.0437.

Jachmann, H., 1988. Estimating age in African elephants: a revision of Laws' molar evaluation technique. African Journal of Ecology, 26 (1), 51-56. http://dx.doi.org/10.1111/j.1365-2028.1988.tb01127.x

Jennings, R. P., Singarayer, J., Stone, E. J., Krebs-Kanzow, U., Khon, V., Nisancioglu, K. H., Pfeiffer, M., Zhang, X., Parker, A., Parton, A., Groucutt, H.S., White, T.S., Drake, N.A., Petraglia, M. D., 2015. The greening of Arabia: Multiple opportunities for human occupation of the Arabian Peninsula during the Late Pleistocene inferred from an ensemble of climate model simulations. Quaternary International 382, 181–199. http://dx.doi.org/10.1016/j.quaint.2015.01.006.

Koepfli, K.-P., Pollinger, J., Godinho, R., Robinson, J., Lea, A., Hendricks, S., Schweizer, R. M., Thalmann, O., Silva, P., Fan, Z., Yurchenko, A. A., Dobrynin, P., Makunin, A., Cahill, J. A., Shapiro, B., Álvares, F., Brito, J. C., Geffen, E., Leonard, J. A., Helgen, K. M., Johnson, W. E., O'Brien, S.J., Van Valkenburgh, B., Wayne, R. K., 2015. Genome-wide evidence reveals that African and Eurasian golden jackals are distinct species. Current Biology 25 (16), 2158-2165. http://dx.doi.org/10.1016/j.cub.2015.06.060.

Kok, O. B., Nel, J. A. J., 1996. The Kuiseb river as a linear oasis in the Namib desert. African Journal of Ecology 34 (1), 39-47. http://dx.doi.org/10.1111/j.1365-2028.1996.tb00592.x.

Kopp, G. H., Roos, C., Butynski, T. M., Wildman, D. E., Alagaili, A. N., Groeneveld, L. F., Zinner, D., 2014. Out of Africa, but how and when? The case of hamadryas baboons (*Papio hamadryas*). Journal of Human Evolution, 76, 154-164. http://dx.doi.org/10.1016/j.jhevol.2014.08.003.

Kurtén, B., 1965. The Carnivora of the Palestine caves. Acta Zoologica Fennica 107. Institute of Zoology and Institute of Geology and Paleontology of the University, Helsingfors, Helsinki.

Larramendi, A., 2015. Shoulder height, body mass and shape of proboscideans. *Acta Palaeontologica Polonica*, http://dx.doi.org/10.4202/app.00136.2014

Laws, R. M., 1966. Age criteria for the African elephant. African Journal of Ecology 4 (1), 1-37. http://dx.doi.org/10.1111/j.1365-2028.1966.tb00878.x.

Lewis, M., Pacher, M., Turner, A., 2010. The larger Carnivora of the West Runton freshwater bed. Quaternary International, 228 (1), 116-135. http://dx.doi.org/10.1016/j.quaint.2010.06.022.

Lister, A. M., 2004. Ecological Interactions of Elephantids in Pleistocene Eurasia: *Palaeoloxodon* and *Mammuthus*. In: Goren-Inbar, N., Speth, J.D. (Eds.), Human Paleoecology in the Levantine Corridor. Oxbow, Oxford, pp. 53-60.

Lister, A. M., 2013. The role of behaviour in adaptive morphological evolution of African proboscideans. Nature 500 (7462), 331-334. http://dx.doi.org/10.1038/nature12275.

Lister. A.M., 2016. Dating the arrival of straight-tusked elephant (Palaeoloxodon spp.) in Eurasia. Bulletin du Musée d'Anthropologie préhistorique de Monaco, année 2015, Supplément n° 6.

Lister, A.M., Dirks, W., Assaf, A., Chazan, M., Goldberg, P., Applbaum, Y.H., Greenbaum, N., Horwitz, L.K., 2013. New fossil remains of *Elephas* from the southern Levant: implications for the evolutionary history of the Asian elephant. Palaeogeography, Palaeoclimatology, Palaeoecology 386, 119-130. http://dx.doi.org/10.1016/j.palaeo.2013.05.013.

Lister, A.M., Sher, A.V., 2015. Evolution and dispersal of mammoths across the northern hemisphere. Science 350, 805-809.

Maglio, V. J., 1973. Origin and evolution of the Elephantidae. Transactions of the American Philosophical Society, 1-149. http://dx.doi.org/10.2307/1006229.

Mallon, D. P., 2011. Global hotspots in the Arabian Peninsula. Zoology in the Middle East 54 (supplement 3), 13-20. http://dx.doi.org/10.1080/09397140.2011.10648896.

Marsh, R.E. 1999. 1Beta-gradient Isochrons Using Electron Paramagnetic Resonance: Towards a New Dating Method in Archaeology. Upublished MSc thesis, McMaster University.

Matter, A., Neubert, E., Preusser, F., Rosenberg, T., Al-Wagdani, K., 2015. Palaeo-environmental implications derived from lake and sabkha deposits of the southern Rub'al-Khali, Saudi Arabia and Oman. Quaternary International 382, 120-131. http://dx.doi.org/10.1016/j.quaint.2014.12.029.

Marciszak, A., 2014. Presence of Panthera gombaszoegensis (Kretzoi, 1938) in the late Middle Pleistocene of Biśnik Cave, Poland, with an overview of Eurasian jaguar size variability. Quaternary International 326-327, 105-113. http://dx.doi.org/10.1016/j.quaint.2013.12.029.

Marean, C.W., Domínguez-Rodrigo, M., Pickering, T.R., 2004. Skeletal Element Equifinality in Zooarchaeology Begins with Method: The Evolution and Status of the "Shaft Critique". Journal of Taphonomy, 2 (2), 69-98.

McClure, H.A., 1984. Late Quaternary Palaeoenvironments of the Rub' al Khali. Unpublished PhD thesis. University College, London.

Metallinou, M., Arnold, E.N., Crochet, P.-A., Geniez, P., Brito, J.C., Lymberakis, P., El Din, S.B., Sindaco, R., Robinson, M., Carranza, S., 2012. Conquering the Sahara and Arabian deserts: systematics and biogeography of *Stenodactylus* geckos (Reptilia: Gekkonidae). BMC evolutionary biology 12 (1), 258. http://dx.doi.org/10.1186/1471-2148-12-258.

Miller, J. M., Hallager, S., Monfort, S.L., Newby, J., Bishop, K., Tidmus, S.A., Black, P., Houston, B., Matthee, C.A., Fleischer, R.C., 2011. Phylogeographic analysis of nuclear and mtDNA supports subspecies designations in the ostrich (*Struthio camelus*). Conservation Genetics 12 (2), 423-431. http://dx.doi.org/10.1007/s10592-010-0149-x.

Morales Muniz A., 1993. Ornithoarchaeology: the various aspects of the classification of bird remains from archaeological sites. Archaeofauna 2, 1-13.

O'Regan, H. J., Bishop, L. C., Lamb, A., Elton, S., Turner, A. 2005. Large mammal turnover in Africa and the Levant between 1.0 and 0.5 Ma. Geological Society, London, Special Publications, 247 (1), 231-249. http://dx.doi.org/10.1144/gsl.sp.2005.247.01.13.

O'Regan, H.J., Turner, A., Bishop, L.C., Elton, S., Lamb, A.L., 2011. Hominins without fellow travellers? First appearances and inferred dispersals of Afro-Eurasian large-mammals in the Plio-Pleistocene. Quaternary Science Reviews 30, 1343-1352. http://dx.doi.org/10.1016/j.quascirev.2009.11.028.

Ostrowski, S., Williams, J.B., Mésochina, P., Sauerwein, H., 2006. Physiological acclimation of a desert antelope, Arabian oryx (*Oryx leucoryx*), to long-term food and water restriction. Journal of Comparative Physiology 176, 191-201. http://dx.doi.org/10.1007/s00360-005-0040-0.

Palombo, M. R., Ferretti, M. P., 2005. Elephant fossil record from Italy: knowledge, problems, and perspectives. Quaternary International, 126, 107-136. http://dx.doi.org/10.1016/j.quaint.2004.04.018.

Parker, A.G., 2009. Pleistocene climate change in Arabia: developing a framework for hominin dispersal over the last 350 ka. In: Petraglia, M.D., Rose, J.I. (Eds.), The Evolution of Human Populations in Arabia: Vertebrate Paleobiology and Paleoanthropology. Springer Netherlands, pp. 39-49. http://dx.doi.org/10.1007/978-90-481-2719-1_3.

Parton, A., Farrant, A.R., Lang, M.J., Telfer, M.W., Groucutt, H.S., Petraglia, M.D., Parker, A.G., 2015a. Alluvial fan records from southeast Arabia reveal multiple windows for human dispersal. Geology 43 (4), 295-298. http://dx.doi.org/10.1130/g36401.1.

Parton, A., White, T.S., Parker, A., Breeze, P.S., Jennings, R., Groucutt, H.S., Petraglia, M.D., 2015b Orbital-scale climate variability in Arabia as a potential motor for human dispersals. Quaternary International 382, 82-97. http://dx.doi.org/10.1016/j.quaint.2015.01.005.

Peters, J., Van Neer, W., Plug, I., 1997. Comparative postcranial osteology of hartebeest (*Alcelaphus buselaphus*), Scimitar oryx (*Oryx dammah*) and Addax (*Addax nasomaculatus*), with notes on the osteometry of Gemsbok (*Oryx gazella*) and Arabian Oryx (*Oryx leucoryx*). Annales Sciences Zoologiques, Vol. 280. Musee Royal de L'Afrique Centrale, Tervuren, 83 pp.

Petraglia, M.D., Alsharekh, A., Breeze, P., Clarkson, C., Crassard, R., Drake, N.A., Groucutt, H.S., Jennings, R., Parker, A.G., Parton, A., Roberts, R.G., Shipton, C., Matheson, C., al-Omari, A., Veall, M.-A., 2012. Hominin dispersal into the Nefud Desert and Middle Palaeolithic settlement along the Jubbah palaeolake, northern Arabia. PLoS ONE 7 (11), e49840. http://dx.doi.org/10.1371/journal.pone.0049840.

Petrucci, M. Romiti, S. Sardella, R., 2012. The Middle-Late Pleistocene *Cuon* Hodgson, 1838 (Carnivora, Canidae) from Italy. Bollettino della Società Paleontologica Italiana 51 (2), 137-148.

Porter, R., Aspinall, S., 2010. Birds of the Middle East (second edition). Christopher Helm, London.

Portik, D. M., Papenfuss, T. J., 2012. Monitors cross the Red Sea: the biogeographic history of *Varanus yemenensis*. Molecular phylogenetics and evolution 62 (1), 561-565. http://dx.doi.org/10.1016/j.ympev.2011.09.024.

Prescott, J. R., Hutton, J., 1988. Cosmic ray and gamma ray dosimetry for TL and ESR. International Journal of Radiation Applications and Instrumentation. Part D. Nuclear Tracks and Radiation Measurements 14 (1), 223-227. http://dx.doi.org/10.1016/1359-0189(88)90069-6.

Prescott, J. R., Hutton, J. T., 1994. Cosmic ray contributions to dose rates for luminescence and ESR dating: large depths and long-term time variations. Radiation measurements 23 (2), 497-500. http://dx.doi.org/10.1016/1350-4487(94)90086-8.

Prescott, J. R., Stephan, L. G., 1982. The contribution of cosmic radiation to the environmental dose for thermoluminescence dating. Latitude, altitude and depth dependences. In Pact 6, 17-25.

Rabinovich, R., Ackermann, O., Aladjem, E., Barkai, R., Biton, R., Milevski, I., Solodenko, N., Marder, O., 2012. Elephants at the Middle Pleistocene Acheulian open-air site of Revadim Quarry, Israel. Quaternary International 276, 183-197. http://dx.doi.org/10.1016/j.quaint.2012.05.009.

Ramey, E.M., Ramey, R.R., Brown, L.M., Kelley, S.T., 2013. Desert-dwelling African elephants (*Loxodonta africana*) in Namibia dig wells to purify drinking water. Pachyderm 53, 66-72.

Readhead, M. L., 2002. Absorbed dose fraction for 87Rb β particles. Ancient TL, 20 (1), 25-28.

Richter, D., Richter, A., Dornich, K., 2013. Lexsyg - A new system for luminescence research. Geochronometria, 40 (4), 220-228. http://dx.doi.org/10.2478/s13386-013-0110-0.

Rivals, F., Semprebon, G., Lister, A., 2012. An examination of dietary diversity patterns in Pleistocene proboscideans (Mammuthus, Palaeoloxodon, and Mammut) from Europe and North America as revealed by dental microwear. Quaternary International 255, 188–195.

Rook, L., Luisa, M., Puccetti, A., Azzaroli, A., 1996. Remarks on the skull morphology of the endangered Ethiopian jackal, *Canis simensis* Rappel 1838. Rendiconti Lincei, 7 (4), 277-302. http://dx.doi.org/10.1007/bf03002246.

Rose, J. I., Petraglia, M. D., 2010. Tracking the origin and evolution of human populations in Arabia. Vertebrate Paleobiology and Paleoanthropology, pp.1–12. Springer Netherlands. http://dx.doi.org/10.1007/978-90-481-2719-1_1.

Rosenberg, T. M., Preusser, F., Fleitmann, D., Schwalb, A., Penkman, K., Schmid, T.W., Al-Shanti, M.A., Kadi, K., Matter, A., 2011. Humid periods in southern Arabia: windows of opportunity for modern human dispersal. Geology 39 (12), 1115-1118. http://dx.doi.org/10.1130/g32281.1.

Rosenberg, T.M., Preusser, F., Risberg, J., Plikk, A., Kadi, K.A., Matter, A., Fleitmann, D., 2013. Middle and Late Pleistocene humid periods recorded in palaeolake deposits of the Nafud desert, Saudi Arabia. Quaternary Science Reviews 70, 109-123. http://dx.doi.org/10.1016/j.quascirev.2013.03.017.

Rueness, E.K., Asmyhr, M.G., Sillero-Zubiri, C., Macdonald, D.W., Bekele, A., Atickem, A., Stenseth, N.C., 2011. The cryptic African wolf: *Canis aureus lupaster* is not a golden jackal and is not endemic to Egypt. PLoS One, 6 (1), e16385. http://dx.doi.org/10.1371/journal.pone.0016385.

Saarinen, J., Karme, A., Cerling, T., Uno, K., Saäilä, L., Kasiki, S., Ngene, S., Obari, T., Mbua, E., Manthi, F.K., Fortelius, M., 2015. A new tooth wear-based dietary analysis method for Proboscidea (Mammalia). Journal of Vertebrate Paleontology 35(3), e918546. http://dx.doi.org/10.1080/02724634.2014.918546.

Saegusa, H., Gilbert, W. H., 2008. Elephantidae. In: Gilbert, H.W., Asfaw, B. (Eds.), Homo erectus in Africa, Pleistocene Evidence from the Middle Awash. University of California Press, Berkeley, pp. 193-226. http://dx.doi.org/10.1525/california/9780520251205.003.0009.

Sanders, W. J., Gheerbrant, E., Harris, J. M., Saegusa, H., Delmer, C., 2010. Proboscidea. In: Werdelin, L., Sanders, W. J. (Eds.), Cenozoic Mammals of Africa. University of California Press, Berkeley, pp. 161-251. http://dx.doi.org/10.1525/california/9780520257214.003.0015.

Sangster, G., Collinson, J. M., Crochet, P. A., Kirwan, G. M., Knox, A. G., Parkin, D. T., Votier, S. C., 2015. Taxonomic recommendations for Western Palaearctic birds: 10th report. Ibis, 157 (1), 193-200. http://dx.doi.org/10.1111/ibi.12221.

Sansalone, G., Bertè, D.F., Maiorino, L., Pandolfi, L., 2015. Evolutionary trends and stasis in carnassial teeth of European Pleistocene wolf *Canis lupus* (Mammalia, Canidae). Quaternary Science Reviews, 110, 36-48. http://dx.doi.org/10.1016/j.quascirev.2014.12.009.

Savioz, N. R., Morel, P., 2005. La faune de Nadaouiyeh Aïn Askar (Syrie centrale, Pléistocène moyen): aperçu et perspectives. Revue de Paléobiologie, Genève, 10, 31-35.

Scerri, E.M.L., Breeze, P.S., Parton, A., Groucutt, H.S., White, T.S., Stimpson, C., Clark-Balzan, L., Jennings, R., Alsharekh, A., Petraglia, M.D., 2015. Middle to Late Pleistocene human habitation in the Western Nefud Desert, Saudi Arabia. Quaternary International, 382, 200-214. http://dx.doi.org/10.1016/j.quaint.2014.09.036.

Sher, A.V., Garutt, V.E., 1987. New data on the morphology of elephant molars. Transactions of the USSR Academy of Sciences, Earth Science Sections 285, 195-199.

Shipton, C., Parton, A., Breeze, P., Jennings, R., Groucutt, H.S., White, T.S., Drake, N., Crassard, R., Alsharekh, A., Petraglia, M.D., 2014. Large Flake Acheulean in the Nefud Desert of Northern Arabia. PaleoAnthropology, 446-462.

Shoshani, J., Tassy, P., 1996. The Proboscidea. Evolution and Palaeoecology of Elephants and Their Relatives. Oxford University Press, Oxford.

Stanley Price, M.R., 1989. Animal re-introductions: the Arabian oryx in Oman. Cambridge University Press, Cambridge.

Stewart, J. R., 2009. The evolutionary consequence of the individualistic response to climate change. Journal of Evolutionary Biology, 22 (12), 2363-2375. http://dx.doi.org/10.1111/j.1420-9101.2009.01859.x.

Stimpson, C.M., Breeze, P.S., Clark-Balzan, L., Groucutt, H.W., Jennings, R., Parton, A., Scerri, E., White, T.S., Petraglia, M.D., 2015. Stratified Pleistocene vertebrates with a new record of a jaguar-sized pantherine (*Panthera* cf. *gombaszogensis*) from northern Saudi Arabia. Quaternary International 382, 168-180. http://dx.doi.org/10.1016/j.quaint.2014.09.049.

Stoyanov, S., 2012. Golden jackal (*Canis aureus*) in Bulgaria. Current status, distribution, demography and diet. In: International symposium on hunting: modern aspects of sustainable management of game population. Zemun-Belgrade, Serbia, pp. 22-24.

Southgate, R.I., Masters, P., Seely, M.K., 1996. Precipitation and biomass changes in the Namib Desert dune ecosystem. Journal of Arid Environments 33, 267-280. http://dx.doi.org/10.1006/jare.1996.0064.

Thiel, C., Buylaert, J. P., Murray, A., Terhorst, B., Hofer, I., Tsukamoto, S., Frechen, M., 2011. Luminescence dating of the Stratzing loess profile (Austria)–Testing the potential of an elevated temperature post-IR IRSL protocol. Quaternary International 234 (1), 23-31. http://dx.doi.org/10.1016/j.quaint.2010.05.018.

Thiel, C., Coltorti, M., Tsukamoto, S., Frechen, M. 2010. Geochronology for some key sites along the coast of Sardinia (Italy). Quat. Int. 222, 36–47. http://dx.doi.org/10.1016/j.quaint.2009.12.020.

Thomas, H., Geraads, D., Janjou, D., Vaslet, D., Memesh, A., Billiou, D., Bocherens, H., Dobigny, G., Eisenmann, V., Gayet, M., de Lapparent de Broin, F., Petter, G., Halawani, M., 1998. First Pleistocene faunas from the Arabian Peninsula: An Nafud desert, Saudi Arabia. Comptes rendues del'Academie des Sciences Paris 326, 145-152. http://dx.doi.org/10.1016/s1251-8050(97)87459-9.

Thomsen, K. J., Murray, A. S., Jain, M., 2011. Stability of IRSL signals from sedimentary K-feldspar samples. Geochronometria 38, 1–13. http://dx.doi.org/10.2478/s13386-011-0003-z.

Tilson, R. L., Henschel, J. R., 1986. Spatial arrangement of spotted hyaena groups in a desert environment, Namibia. African Journal of Ecology 24 (3), 173-180. http://dx.doi.org/10.1111/j.1365-2028.1986.tb00358.x.

Todd, N. E., 2001. African *Elephas recki*: time, space and taxonomy. In: Cavarretta, G., Giola, P., Mussi, M., Palombo, M.R. (Eds.), The World of Elephants, Proceedings of the 1st International Congress. Consiglio Nazionale delle Ricerche, Rome, pp. 693-697.

Trauerstein, M., Lowick, S., Preusser, F., Rufer, D., Schlunegger, F., 2012. Exploring fading in single grain feldspar IRSL measurements. Quaternary Geochronology 10, 327-333. http://dx.doi.org/10.1016/j.quageo.2012.02.004.

Valeix, M., Loveridge, A.J., Davidson, Z., Madzikanda, H., Fritz, H., Macdonald, D.W., 2010. How key habitat features influence large terrestrial carnivore movements: waterholes and African lions in a semi-arid savanna of north-western Zimbabwe. Landscape Ecology 25, 337-351. http://dx.doi.org/10.1007/s10980-009-9425-x.

Viljoen, P.J., 1989a. Habitat selection and preferred food plants of a desert-dwelling elephant population in the northern Namib Desert, South West Africa/Namibia. African Journal of Ecology 27, 227-240. http://dx.doi.org/10.1111/j.1365-2028.1989.tb01016.x.

Viljoen, P.J., 1989b. Spatial distribution and movements of elephants (*Loxodonta africana*) in the northern Namib Desert region of the Kaokoveld, South West Africa/Namibia. Journal of Zoology 219, 1-19. http://dx.doi.org/10.1111/j.1469-7998.1989.tb02561.x.

van Asperen, E. N., Stefaniak, K., Proskurnyak, I., Ridush, B., 2012. Equids from Emine-Bair-Khosar Cave (Crimea, Ukraine): co-occurrence of the stenonid Equus hydruntinus and the caballoid E. ferus latipes based on skull and postcranial remains. Palaeontologia Electronica, 15 (1), 5A.

Vekua, A., 2013. Giant ostrich in Dmanisi Fauna. Bulletin of the Georgian National Academy of Sciences 7 (2), 143-148.

Von Den Driesch, A., 1976. A guide to the measurement of animal bones from archaeological sites: as developed by the Institut für Palaeoanatomie, Domestikationsforschung und Geschichte der Tiermedizin of the University of Munich (Vol. 1). Peabody Museum Press.

Whybrow, P. J., Hill, A. P. (Eds.), 1999. Fossil vertebrates of Arabia: with emphasis on the late Miocene faunas, geology, and palaeoenvironments of the Emirate of Abu Dhabi, United Arab Emirates. Yale University Press.

1713 Zimmerman, D. W., 1971. Thermoluminescent dating using fine grains from pottery. Archaeometry. 13, 29-52.
1714 http://dx.doi.org/10.1111/j.1475-4754.1971.tb00028.x.
1715
1716
1717
1718
1719
1720
1721
1722
1723